

**NOTICE: THIS
MATERIAL MAY
BE PROTECTED
BY COPYRIGHT
LAW (TITLE 17
U.S. CODE).**

DOSIMETRY OF PARTICLES IN LABORATORY ANIMALS AND HUMANS IN RELATIONSHIP TO ISSUES SURROUNDING LUNG OVERLOAD AND HUMAN HEALTH RISK ASSESSMENT: A Critical Review

Frederick J. Miller

Chemical Industry Institute of Toxicology, Research Triangle Park,
North Carolina, USA

For most compounds, the database for assessing potential risk to humans largely comes from animal toxicology studies. Toxicologists and risk assessors are faced with a series of judgments when deciding whether to use the animal data and then with various extrapolations if the animal results are used. The current workshop is focused on assessing the relevance of the rat as a model for hazard and risk characterization of inhaled, poorly soluble, nonfibrous, nongenotoxic particles of low toxicity (hereafter referred to as poorly soluble particles, PSP). The impetus for the assessment stems from the fact that such materials appear to only produce tumorigenic responses, and then only in the rat when alveolar macrophage (AM)-mediated particle clearance is overwhelmed and chronic inflammation is present. Other workshop critical review papers are addressing aspects related to homology (the nature of the rat lung tumors and their potential counterpart in humans) as well as the types of nonneoplastic responses seen in laboratory animals and the potential mechanisms responsible for these effects. This review examines factors governing the dosimetry of inhaled particles in laboratory animals and humans and how complex interactions among these factors influence the inhalability, deposition, and clearance of particles as well as their temporal translocation and retention within the body.

The factors governing the dosimetry of particles can be broadly grouped into two categories, one dealing with the physicochemical properties of the particles and the other with species-specific factors such as airway structure, ventilatory level, and mucociliary clearance and alveolar rates.

Report from the ILSI Workshop on the Relevance of the Rat Lung Response to Particle Overload for Human Risk Assessment, 23–24 March 1998. Accepted 16 April 1999.

The author thanks Annie Jarabek of the U.S. Environmental Protection Agency for her assistance in obtaining various tables and figures from the chapter on dosimetry of inhaled particles in the Agency's *Air Quality Criteria for Particulate Matter* document. The author also expresses appreciation to the authors of that dosimetry chapter for their comprehensive review of the literature; their excellent work enabled this author to cite, extract, and/or paraphrase information on the findings of various investigators without having to "track down" the original citations.

Address correspondence to Dr. Frederick J. Miller, Chemical Industry Institute of Toxicology, 6 Davis Drive, PO Box 12137, Research Triangle Park, NC 27709, USA. E-mail: fmiller@ciit.org

While particle dissolution rate and chemical composition are important physicochemical properties for the toxicity of many particles, they are basically unimportant for the dosimetry of PSP, such as carbon black, coal, diesel soot, talc, and titanium dioxide, that are the focus of this review. Particle size, density, and distribution will prove to be important physical properties for the aforementioned particles.

For the purpose of this review, dosimetry refers to estimating or measuring the amount (mass, or number, surface area, volume, etc.) of PSP at specific target sites at a particular point in time. This encompasses both deposition, which is the process of removing particles in various regions of the respiratory tract during the breathing of particle-laden air, and clearance, which refers to the rates and routes by which deposited particles are removed from the respiratory tract. Typically, the term "retained dose" in particulate inhalation studies refers to the amount of particles present at specific respiratory tract sites that is the net difference between deposition and clearance processes.

Experimental data on the deposition of particles are usually obtained from exposures lasting minutes to at most a few hours. In contrast, clearance data are obtained by measurements made days to many weeks after the cessation of exposure. Estimates of retained dose arise when body burden measurements are made serially with time as inhalation exposures are continued. Chronic exposures result in respiratory tract burdens that continue to increase over time until the rate of deposition is offset by the rate of clearance, thereby resulting in a steady-state burden from that time on. Body burden patterns differ among species. Higher exposure levels lead to higher steady-state burdens (see Figure 1). Curve C* of Figure 1 illustrates the type of retained lung burden seen with excessively high exposures that lead to impairment of AM-mediated particle clearance resulting in "lung overload." The breakpoint where retained lung burden of PSP starts to depart from the steady-state curve (C of Figure 1) is inversely related to the magnitude of the exposure concentration.

MECHANISMS OF DEPOSITION

Laws of physics govern the transport of particles entrained in the air. Particle transport and physical properties of the particles combine to yield mechanisms by which particles are removed from the airstream. The nature of the major mechanisms of deposition are described prior to discussing the regions of the respiratory tracts of animals and humans in which the various mechanisms predominate.

The major mechanisms by which noncharged particles deposit are inertial impaction, sedimentation, and diffusion (Brownian). These mechanisms are illustrated schematically in Figure 2. Electrostatic attraction may be an important mechanism for the deposition of poorly soluble particles in some workplace exposure settings if the processes being used

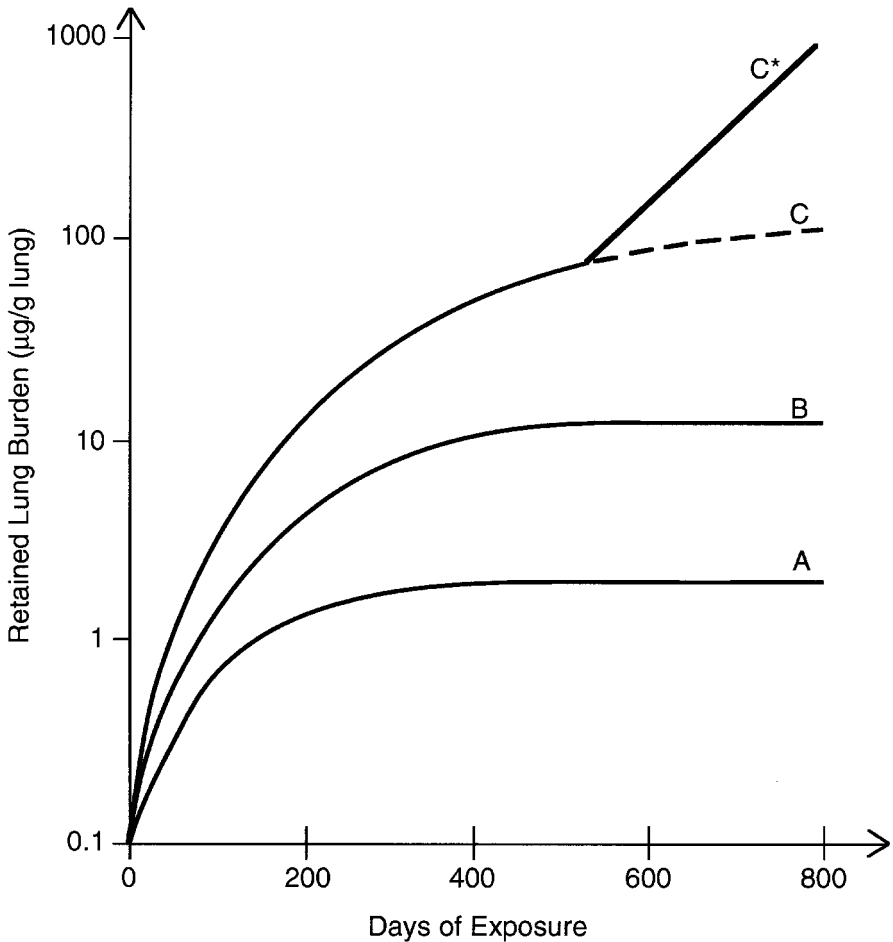


FIGURE 1. Schematic representation of the relationship between retained lung burden and length of exposure leading to the phenomenon of lung overload. Curves A, B, and C are associated with progressively increasing exposure concentrations. If the exposure level is sufficiently high and the length of exposure sufficiently long, alveolar macrophage-mediated clearance of particles can be overwhelmed. When this occurs, retained lung burden increases linearly with further exposure (curve C*).

generate charged particles and workers are in close proximity to the sources of these particles. However, electrostatic attraction is not an important deposition mechanism for ambient exposures to particles since there is ample time for such aerosols to come to Boltzman equilibrium. Inertial impaction is the process by which the inertia of the particle makes it unable to follow changes in the airstream direction or air velocity streamlines. Sedimentation refers to the settling out of particles from the airstream due to gravitational forces. The random displacement motion of particles resulting from constant bombardment by air molecules (Brownian diffusion) can result in particles coming into close proximity of airway

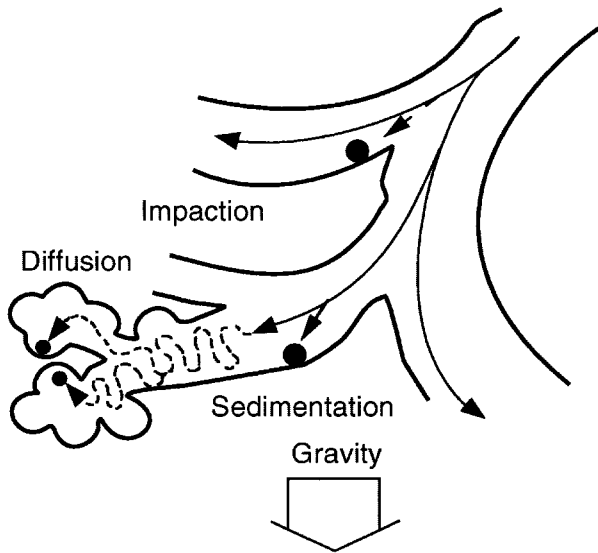


FIGURE 2. Primary mechanisms of deposition of inhaled noncharged particles in the respiratory tract. Streamline, solid lines; particle trajectory, dashed lines. Modified from McClellan and Miller (1997).

surfaces. Depending upon particle size and airflow rate, diffusion, sedimentation, and impaction do not necessarily act as independent processes. Once particles are brought in close proximity to the airway walls, they are removed from the airstream by interception with the walls. Because objects that are relatively long compared to their diameter have an increased probability of the ends intercepting the wall of an airway, interception is often considered by some as a separate deposition mechanism for fibers.

The geometric (physical or diffusion equivalent) and aerodynamic equivalent diameters of a particle are important determinants of the relative importance of these mechanisms in the deposition of particles. Aerodynamic diameter (d_{ae}) takes into account the size, shape, and density of a particle and is defined to be the diameter of a unit-density (1 g/cm^3) sphere having the same terminal settling velocity as the particle. Since particles of different sizes and density can have the same d_{ae} , they can be deposited in the same locations within the respiratory tract.

RESPIRATORY-TRACT STRUCTURE AND FUNCTION

The respiratory tract can be subdivided into three main regions: the extrathoracic (ET) (from the nose and mouth down to and including the larynx); the tracheobronchial tree (trachea to terminal bronchioles); and the pulmonary region (respiratory bronchioles to terminal alveolar sacs). Among disciplines, different nomenclature is often used for these regions.

For example, the upper respiratory tract (URT) is the same as the ET region; pulmonary (P) and alveolar (A) are used interchangeably. Also, the tracheo-bronchial (TB) region is often referred to as the conducting airways. The lower respiratory tract (LRT) is comprised of the TB and A regions and is also referred to as the thoracic region. The anatomical or structural features of each of the major regions differ significantly among laboratory animals and humans on both macro- and microscopic scales. Table 1 provides a synopsis of key aspects of the morphology, cytology, histology, function, and structure of the respiratory tract of rats and humans. In the sections that follow, the structure and function of each region are briefly discussed, and some insights are provided as to which mechanisms of particle deposition are important in the given region.

ET Structure and Function

In the ET region, the inhaled air is conditioned with respect to temperature and humidity (Proctor & Anderson, 1982), and there is an active mucociliary system for the removal of foreign solid material (Phipps, 1981). Similarities between rats and humans also extend to the cytology of the ET epithelium and the histology of the ET airway walls. The same four types of epithelium (squamous, transitional, respiratory, and olfactory) are present in both species, although the percent of the ET covered by the types of epithelium differs among species (Harkema, 1992).

Probably the most significant differences in respiratory structure between rats and humans occur in the URT. Cross sections of the nasal passages of these two species shown in Figure 3 illustrate the nature of the differences. Bulk airflow patterns are influenced by these complex structures such that major medial and lateral airflow streams are formed in the nose of the rat (Morgan et al., 1991; Kimbell et al., 1993) that are quite different from those in humans (Hahn et al., 1993; Subramaniam et al., 1998). The tortuous nasal passages result in inertial impaction being the predominant mechanism by which inhaled particles larger than about 5 μm are deposited in the head of both rats and humans. In addition, ultra-fine particles ($<0.1 \mu\text{m}$ in diameter) are effectively removed in the nose via diffusion since the surfaces of the nasal turbinates are large compared to the cross-sectional area and are in close proximity to the inhaled air.

TB Structure and Function

The main function of the TB region of all mammalian species is to deliver oxygen efficiently to the alveolar region where gas exchange (oxygen for carbon dioxide) occurs. The types of cells comprising the TB epithelium are similar to those contained in the transitional and respiratory epithelium of the ET region. However, there are significant differences between rats and humans in the number of any given cell type as a function of airway size (Mercer et al., 1994b). The liquid layer lining the conducting airways contains mucus. The liquid lining layer protects the tissue from direct expo-

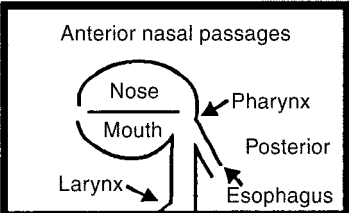
TABLE 1. Key aspects of the structure and function of the respiratory tract of rats and humans

Functions	Cytology (epithelium)	Histology (walls)
Air conditioning: temperature and humidity, and cleaning; fast particle clearance; air conduction	Epithelium types: Squamous Transitional Respiratory Olfactory	Mucous membrane, respiratory epithelium (pseudostratified), ciliated, mucous), glands
	Cell types: Ciliated cells: Nonciliated cells: Goblet cells Mucous (secretory) cells Serous cells Brush cells Endocrine cells Basal cells Intermediate cells	Mucous membrane, respiratory or stratified epithelium, glands Mucous membrane, respiratory epithelium cartilage rings, glands Mucous membrane, respiratory epithelium, cartilage plates, smooth muscle layer, glands
	Respiratory epithelium with clara cells (no goblet cells)	Mucous membrane, respiratory epithelium, no cartilage, no glands, smooth muscle layer
	Cell types: Ciliated cells Nonciliated cells Clara (secretory) cells	Mucous membrane, single- layer respiratory epithelium, less ciliated, smooth muscle layer
	Respiratory epithelium consisting mainly of Clara cells (secretory) and few ciliated cells	Mucous membrane, single- layer respiratory epithelium of cuboidal cells, smooth muscle layer
Gas exchange; very slow particle clearance	Squamous alveolar epithelial cells (type I), covering 97% of alveolar surface areas	Wall consists of alveolar entrance rings, squamous epithelial layer, surfactant
	Cuboidal alveolar epithelial cells (type II, surfactant-producing), covering 3% of alveolar surface area Alveolar macrophages	Interalveolar septa covered by squamous epithelium, containing capillaries, surfactant

Note. Table modified from U.S. Environmental Protection Agency (1996).

sure to inhaled pollutants and is composed of an epiphase and an underlying hypophase in which cilia beat in a manner that propels mucus to the glottis, where it is swallowed. For information on the comparative biochemistry of this layer, the reader is referred to Hatch (1992).

The thickness of the mucociliary layer varies as a function of location within the TB region. For rats and humans, Table 2 gives available data on

Anatomy	Zones (air)	Location	Comments
		Extrathoracic	Rats are obligate nasal breathers. Adult humans switch to oronasal breathing when minute ventilation exceeds about 35 L min ⁻¹ (Niinimaa et al., 1981).
Trachea	Conduction	Thoracic Tracheo- bronchial	Rat lung has predominantly a monopodial branching system (Crapo et al., 1990).
Main bronchi			
Bronchi			
Bronchioles	Gas exchange	Alveolar transitory	Rats do not have respiratory bronchioles. From the bronchiolar-alveolar duct junction in a rat, alveolar sacs are reached after anywhere from 3 to 13 branchings (Mercer & Crapo, 1987).
Terminal bronchioles			
Respiratory bronchioles			
Alveolar ducts			
Alveolar sacs			
Lymphatics			

the thickness of the liquid lining layer in the TB and ET regions and on mucous velocities. The mean mucous velocities given in Table 2 have associated with them relatively large standard deviations. As noted by Wolff (1992), mucous clearance is not necessarily as relentless and uniform as one might be led to believe, particularly in view of the fact there are preferential routes of clearance. Thus, some deposited particles may

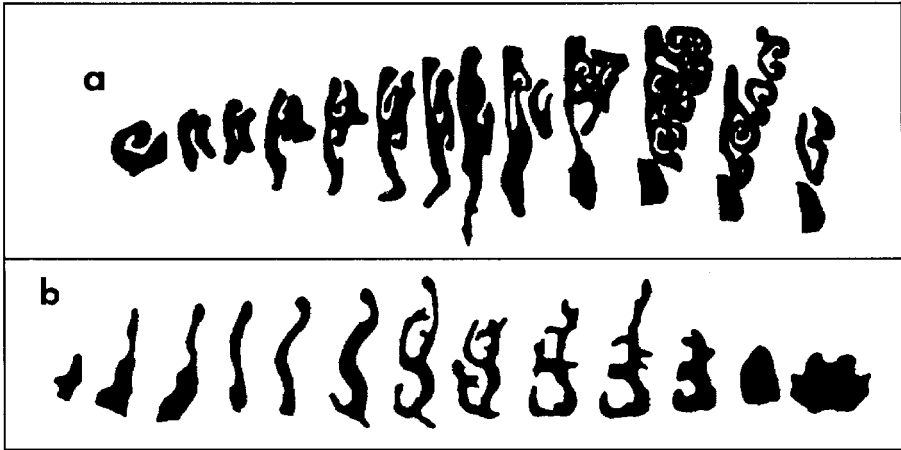


FIGURE 3. Aspects of upper respiratory tract structure important for dosimetry. (a) Cross sections of one side of the rat nasal passages, nostril at left. (b) Cross sections of one side of the human nasal passages, nostril at left. From Miller and Kimbell (1995).

be retained in areas of slow clearance for extended periods of time. The extent to which rats and humans may differ in this regard is not known. Observations in humans (Goodman et al., 1978) and in rats (Wolff et al., 1987) that mean tracheal mucous velocities decline with increasing age have important implications for assessing the risks of relatively insoluble particles, particularly if comparable reductions in mucociliary clearance are also occurring in smaller TB airways.

The structure of the TB region at the gross level can be thought of as a complex branching system of tubes or pipes. The anatomical depiction in Table 1 of the TB airways of humans corresponds to a symmetric branching system denoted as regular and dichotomous, since each branching parent tube gives rise to two daughter tubes of the same diameter. This corresponds to the lung model developed by Weibel (1963) and represents the lung structure most often used in human dosimetry models for both gases and particles. In actuality, the conducting airways of humans exhibit an irregular bipodial and tripodial branching pattern (Crapo et al., 1990). Despite this, when Martonen (1983) compared the results obtained using symmetric TB geometries (Weibel, 1963; Soong et al., 1979) or the asymmetric model of Horsfield et al. (1971), he found that the symmetric models gave better agreement with the available human experimental deposition data than did the asymmetric model.

The TB airways in the rat lung have predominately a monopodial branching system (Crapo et al., 1990). In rats, terminal bronchioles can be reached after anywhere from 7 to 32 branchings, whereas in the human lung from 10 to 22 branchings may be needed before reaching a terminal bronchiole (Yeh & Harkema, 1993). The difference between the TB airway branching systems of rodents and primates is illustrated schemat-

TABLE 2. Tracheobronchial and ET liquid lining layer thickness and mucous velocities

Species	Location	Thickness ^a (μm)	Comments	Reference	Mucous velocity (mm/min)	Reference
Human	Nose				5.2 \pm 2.3 to 8.4 \pm 4.8	van Ree and van Dishoeck (1962) Andersen et al. (1971)
	Trachea				3.6 \pm 1.5 to 21.5 \pm 5.5	Yeates et al. (1975) Santa Cruz et al. (1974)
	Bronchi (main stem)	8.3 ^b	Combination of airway and vascular fixation,	Mercer et al. (1992)		
	Bronchi (segmental) Bronchioles	6.9 ^b 1.8 ^b	lobes were surgical resections in nonsmokers (for methods, see Mercer & Crapo, 1987)			
Rat	Nose	≤ 15	Observed a continuous blanket	Luchtel (1976) Morgan et al. (1984)	2.3 \pm 0.8	Dahl et al. (1986)
					1.1 to 5.9 (respiratory epithelium) 0.9 (olfactory epithelium)	Morgan et al. (1986)
	Trachea, large bronchi Trachea Lobar bronchi	5-10 3-15 Generally 8-12 ^b Few tenths-8 Generally 2-5 ^b	"Distribution was focal" Mucous blanket observed	Yoneda (1976) Luchtel (1978)	1.9 \pm 0.7 to 5.9 \pm 2.5	Felicetti et al. (1981) Giordano and Morrow (1972)

(Table continues on next page)

TABLE 2. Tracheobronchial and ET liquid lining layer thickness and mucous velocities (*continued*)

Species	Location	Thickness ^a (μm)	Comments	Reference	Mucous velocity (mm/min)	Reference
Rat (<i>cont.</i>)	Trachea	6.1 ^b	Combination of airway and vascular fixation (for methods, see Mercer & Crapo, 1987)	Mercer et al. (1992)		
	Bronchi	3 ^b				
	Bronchioles	2 ^b				
	Terminal bronchioles Trachea, major bronchi, peripheral airways	0.0	No epiphase or mucus observed: "Well defined streams up to 500 mm wide." "Mucus was transported as discrete particles" as small as 0.5 mm in diameter. A continuous mucous blanket was not observed.	Iravani and van As (1972) Stephens et al. (1974) van As and Webster (1972, 1974)		

^aUnless specified, values apply only to the epiphase above cilia tips.

^bThickness of epiphase plus hypophase.

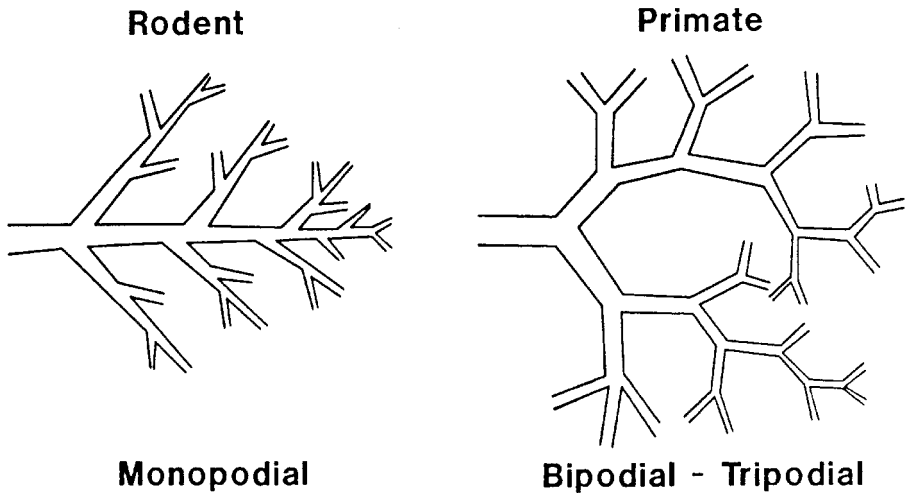


FIGURE 4. Illustration of short and long pathway models for reaching the gas-exchange region in either a monopodial or a bipodial/tripodial airway branching system. From Crapo et al. (1990).

ically in Figure 4. The branching differences are particularly important relative to the sites of deposition of inhaled particles. Impaction is the predominant mechanism for particle deposition in the TB airways of humans for particles greater than $2.5 \mu\text{m } d_{ae}$; both impaction and sedimentation are important for deposition of particles greater than $1 \mu\text{m } d_{ae}$ in the TB airways of laboratory animals. Since mean flow rate and residence time influence impaction and sedimentation, respectively, impaction is even more significant for TB deposition as humans engage in activities that increase their minute ventilation. In humans and rats, enhanced deposition of particles larger than $2.5 \mu\text{m}$ during inspiration occurs at airway bifurcations (Martonen & Hofmann, 1986; Schlesinger, 1989). With expiration, there is a tendency in humans for increased deposition on the walls of the parent tube within a distance of about one diameter of the airway size, while the monopodial branching system of the rat tends to impart increased deposition on the parent wall opposite the opening of the smaller daughter airway (Schlesinger, 1989). Also, the turbulence created by the laryngeal jet tends to result in enhanced deposition of ultrafine particles ($<0.1 \mu\text{m}$ in geometric diameter) in the trachea and larger TB airways due to diffusion (Cohen, 1987; Cohen et al., 1990).

Alveolar Region Structure and Function

Since the alveolar region is where gas exchange occurs, a teleological argument has often been made that the types of cells in this region should be essentially the same in various mammalian species. The work of Stone and colleagues (1992) amply demonstrated that there is significant structural homogeneity of alveolar cells in mammals ranging over more than five orders of magnitude in body weight (i.e., from the shrew to the

horse). The larger surface area of the human lung arises from more, not necessarily larger, cells than are in the alveolar region of the rat. Given the larger amount of tissue to support as the lung increases in size, there is a corresponding linear increase in both collagen and elastin-rich fiber systems as the body weight of mammalian species increases (Mercer & Crapo, 1990). However, since collagen and elastin fibers are concentrated at alveolar entrance rings, Mercer and Crapo (1990) found that the normalized volume density of collagen and elastin fibers at these locations was 10-fold greater in humans compared to mice, despite the fact that an alveolus in a human lung is only 4-fold larger than the alveolus in a mouse. The role these differences may play among species in fibrotic responses caused by prolonged exposure to relatively insoluble particles is unknown.

The liquid layer lining the alveolar epithelium is comprised of surfactant, which contains a number of surface-active materials, primarily phospholipids. Surfactant lowers the work of breathing by lowering surface tensions, thereby stabilizing alveoli and preventing them from collapsing. The surfactant layer is nonuniform in that there is a thin film ($<0.01 \mu\text{m}$ thick) on a hypophase approximately 10 times thicker, but there is significant pooling of surfactant in corners (pockets) of alveoli during expiration. The phospholipid composition of lung surfactant is remarkably similar between rats and humans (see Table 7 of Rooney, 1992). Since airflow reduces with each bifurcation of the airways, airflow in the alveolar region is low and is essentially laminar. Even at flow rates 10–15 times greater than needed for normal respiration, convection is only 12% as important as diffusion for gas transport (Davidson & Fitz-Gerald, 1974). As a result, diffusion is the primary mechanism by which particles $<0.5 \mu\text{m}$ entrained in air that reaches the alveolar region are deposited. For particles $>1 \mu\text{m}$ d_{ae} , sedimentation is the dominant mechanism for alveolar region deposition.

The material presented thus far clearly demonstrates that the complex interactions among species-specific respiratory tract anatomy, the route and depth of breathing, and particle-specific physical factors determine the sites of deposition of particles at various locations within the respiratory tract (see Figure 5). In addition, the relative importance of the major mechanisms by which deposition occurs is influenced by these factors. For both rats and humans, impaction predominates in the ET region, while diffusion largely governs deposition in the alveolar region. The relative importance of impaction and sedimentation varies significantly between rats and humans, primarily due to differences in airway size and overall lung architecture. Both processes are important for TB deposition in rats, but impaction is the predominant mechanism for TB deposition in humans.

EXPERIMENTAL DATA ON REGIONAL DEPOSITION

A number of experimental studies on the regional deposition of particles have been conducted using healthy, adult human subjects. Much less

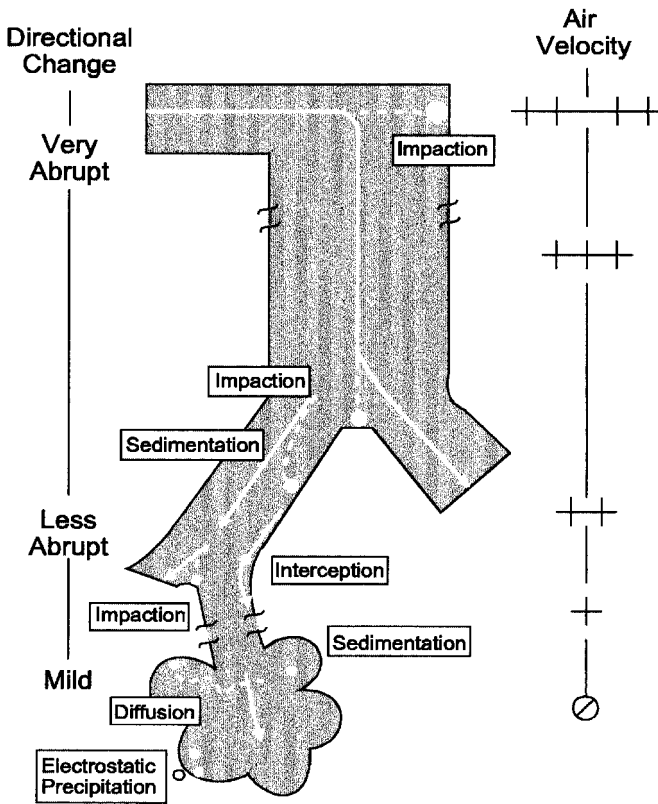


FIGURE 5. Schematic representation of major mechanism governing the deposition of particles in the respiratory tract. Airflow is signified by the arrows and particle trajectories by the dashed lines. Figure modified from U.S. Environmental Protection Agency (1996).

data are available from animal studies specifically designed to determine regional deposition of particles. For a detailed review of these studies, the reader is referred to Chapter 10 of the U.S. Environmental Protection Agency (EPA) recent document on Air Quality Criteria for Particulate Matter (U.S. Environmental Protection Agency, 1996). Here, overall trends in deposition are briefly reviewed.

ET Region Deposition

Recall that impaction is the predominant mechanism for deposition of particles in the ET region and that humans breathe through both the nose and the mouth depending upon activity level or medical condition. Thus, an impaction parameter, $d_{ae}^2 Q$, where Q is the inspiratory flow rate, is used to relate deposition efficiency when breathing through the nose (Figure 6) as compared to the mouth (Figure 7). Several conclusions are apparent from the data shown in Figures 6 and 7. They are: (1) There is a tremendous increase in variability in deposition efficiency as values of the

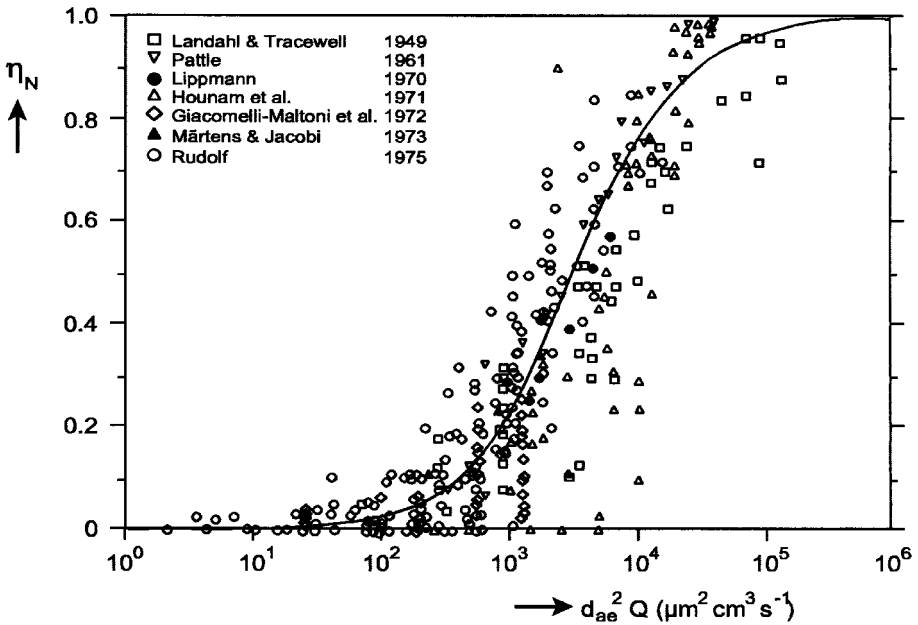


FIGURE 6. Inspiratory deposition of the human nose as a function of particle aerodynamic diameter and flow rate ($d_{ae}^2 Q$). The curve represents the equation $\eta_n = 1 - [3.0 \times 10^{-4} (d_{ae}^2 Q) + 1]^{-1}$. Data are from Stahlhofen et al. (1989), and equation is from the International Commission on Radiological Protection (1994).

impaction parameter increase from 100 to 10,000 $\mu\text{m}^2 \text{cm}^3 \text{s}^{-1}$ for nasal breathing; (2) since the size of the ET region during mouth breathing increases with increasing flow rate and tidal volume, the empirical equation fit to the deposition efficiency data for mouth breathing is of a different form than that used for nasal breathing; (3) as with nasal breathing, there is significant scatter in the experimental data for ET deposition when inhaling through the mouth; and (4) nasal breathing is considerably more efficient in removing inhaled particles than is oral breathing.

Experimental data on the deposition of particles in the ET region of various laboratory animals are shown in Figure 8. Overall, there is less variability in ET deposition of particles in animals compared to humans.

TB Region Deposition

Particles that penetrate the ET region can be deposited in TB airways. Only an indirect assessment of deposition in this region is possible in human experimental studies. Since the experimental studies use radio-labeled PSP, the amount of activity retained in the lung as a function of time is determined; then TB deposition is derived from the fast decay component (i.e., the first 24 h) of the activity curve, with alveolar deposition being estimated from the slow decay portion of the activity curve. The rationale for this approach to determining TB and A deposition is that the fast

and slow decay components are considered to represent mucociliary and macrophage clearance, respectively. However, the cutpoint of 24 h for TB airway deposition is somewhat arbitrary, as there is experimental evidence in support of the concept that some material deposited in the TB region is retained considerably longer than 24 h (Scheuch & Stahlhofen, 1988). The factors responsible for this observation have not been elucidated, although phagocytosis by airway macrophages, an incomplete mucous layer, and flow mixing have all been postulated as potentially being involved. Whatever the reason, it is likely operative in rats as well as humans.

Experimental data for TB deposition of particles in humans are shown in Figure 9. Of note is that the data in Figure 9 represent deposition fractions rather than deposition efficiencies. While deposition fractions and efficiencies are the same for the ET region, the same cannot be said for the TB region. If the deposition data were expressed as the number of particles depositing in the TB region divided by the number of particles entering the TB region, the result would be TB deposition efficiencies, which would asymptotically approach one as particle size increased. For a discussion of the relationship between deposition fractions and efficiencies and how they can be calculated for the ET, TB, and A regions, the reader is referred to Ménache et al. (1996).

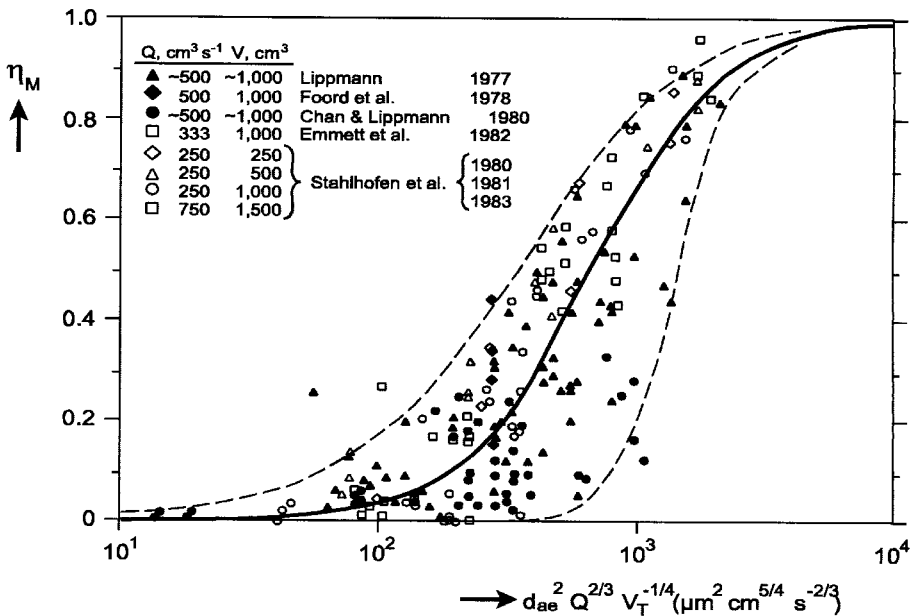


FIGURE 7. Inspiratory extrathoracic deposition data in humans during mouth breathing as a function of particle aerodynamic diameter, flow rate, and tidal volume ($d_{ae}^2 Q^{2/3} V_T^{-1/4}$). The solid curve represents the equation $\eta_N = 1 - [1.1 \times 10^{-4} (d_{ae}^2 Q^{0.6} V_T^{-0.2})^{1.4} + 1]^{-1}$, with the dashed lines representing 95% confidence limits on the mean. Data are from Stahlhofen et al. (1989), and the equation is from the International Commission on Radiological Protection (1994).

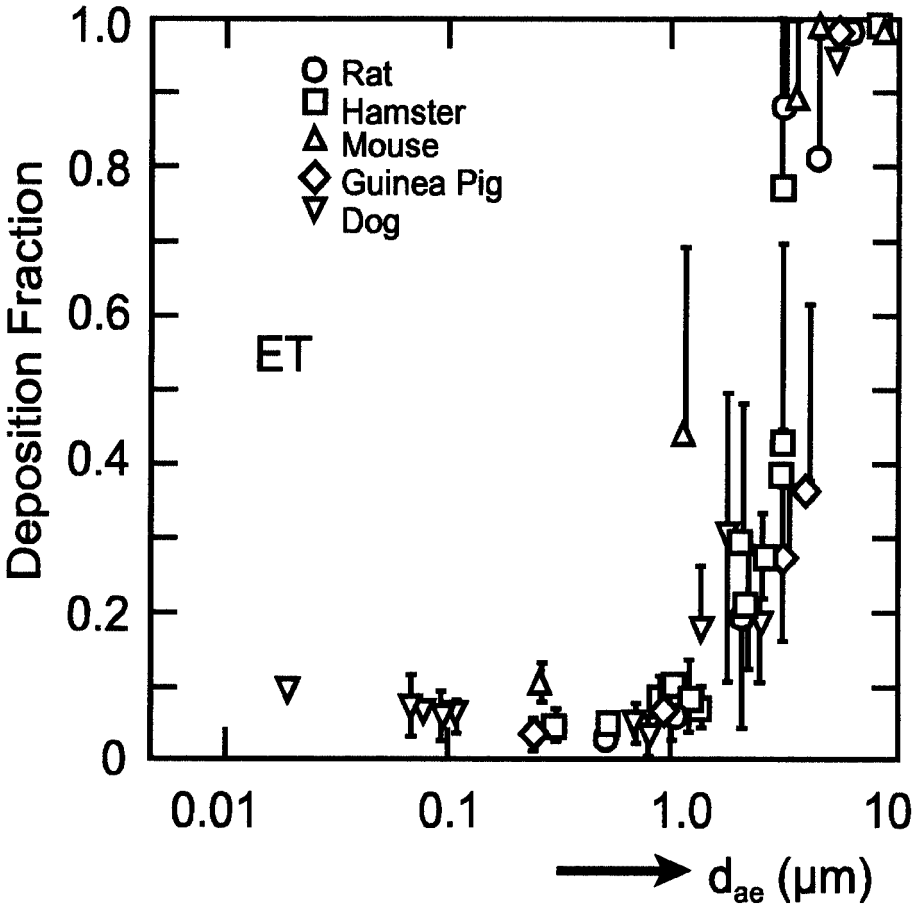


FIGURE 8. Extrathoracic (ET) deposition fractions in various animal species as a function of particle aerodynamic diameter. For those smaller than $0.5 \mu\text{m}$, geometric diameters were used. The data are from Schlesinger (1988).

Considerable scatter can be seen in the TB deposition data in Figure 9. This scatter is due to differences in (1) experimental techniques, (2) intra- and intersubject variability, and (3) flow rates used in the various studies, coupled with the fact that d_{ae} is used on the abscissa. Since impaction is directly proportional and sedimentation is inversely proportional to flow rate, a single relationship between deposition and d_{ae} for different flow rates is not possible. Hence, combining data from experiments using different flow rates as was done in Figure 9 will automatically impart scatter. The peak deposition fraction in the TB region occurs for particles about $4 \mu\text{m}$ d_{ae} . Also, note that there is very modest deposition in the TB region for particles $<1 \mu\text{m}$ d_{ae} . Regional respiratory tract experimental data are not currently available for TB deposition of ultrafine particles (i.e., particles with a physical diameter $<0.1 \mu\text{m}$). Dosimetry models predict deposition fractions to approach a peak of 0.6 for $0.005 \mu\text{m}$ particles

and then to decrease as particle size decreases (International Commission on Radiological Protection, 1994). However, TB deposition studies of ultra-fines in human replica cast (Cohen, 1987; Cohen et al., 1990) yield deposition efficiencies that are about twofold higher than those predicted using dosimetry models.

Data on the fraction of particles deposited in the TB region of rats, hamsters, mice and other animal species are shown in Figure 10. TB deposition is minimal, being typically 5–10%, and is essentially uniform across these species for particles $>0.5 \mu\text{m } d_{ae}$ at least within the error of measurement. Since there is nearly complete ET deposition of particles $>4 \mu\text{m } d_{ae}$ in rodents, TB deposition of such particles is correspondingly low.

Alveolar Region Deposition

Alveolar deposition fractions in healthy, adult humans as a function of d_{ae} are shown in Figure 11. As with other regional deposition data, significant scatter is depicted. For particles $>1 \mu\text{m } d_{ae}$, there is enhanced alveolar deposition when individuals breathe through the mouth as compared to the nose, as indicated by the solid and dashed lines, respectively. Below $1 \mu\text{m } d_{ae}$ the two routes of breathing yield similar alveolar deposition fractions. The peak for alveolar deposition occurs at a d_{ae} of about $3.5 \mu\text{m}$.

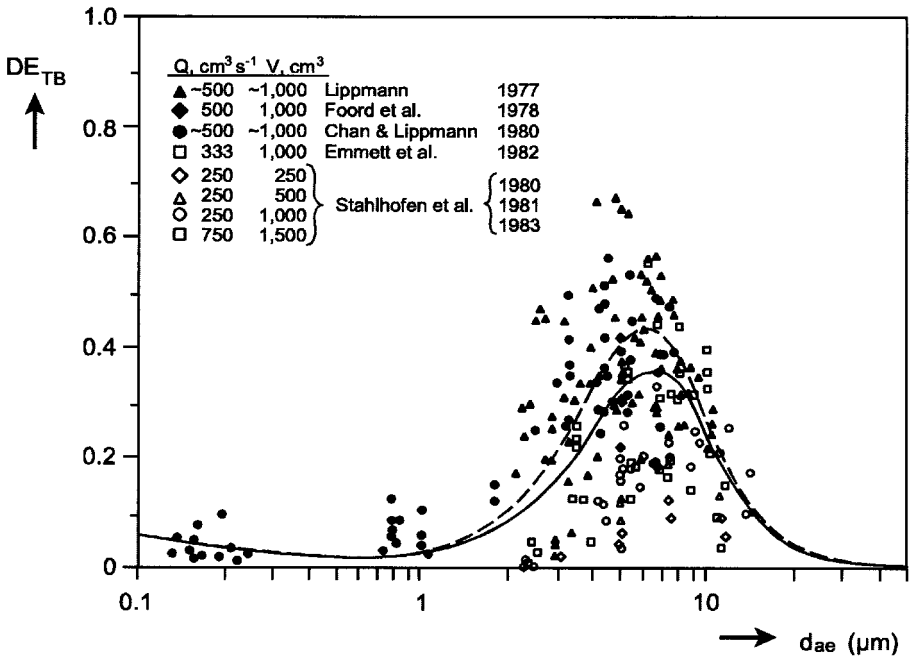


FIGURE 9. Tracheobronchial deposition data in humans at mouth breathing as a function of particle aerodynamic diameter (d_{ae}). Here, DE_{TB} represents the fraction of particles depositing in the TB region out of the total inhaled. The solid curve represents the approximate mean of all the experimental data; the broken curve represents the mean excluding the data of Stahlhofen and colleagues. Data are from Stahlhofen et al. (1989).

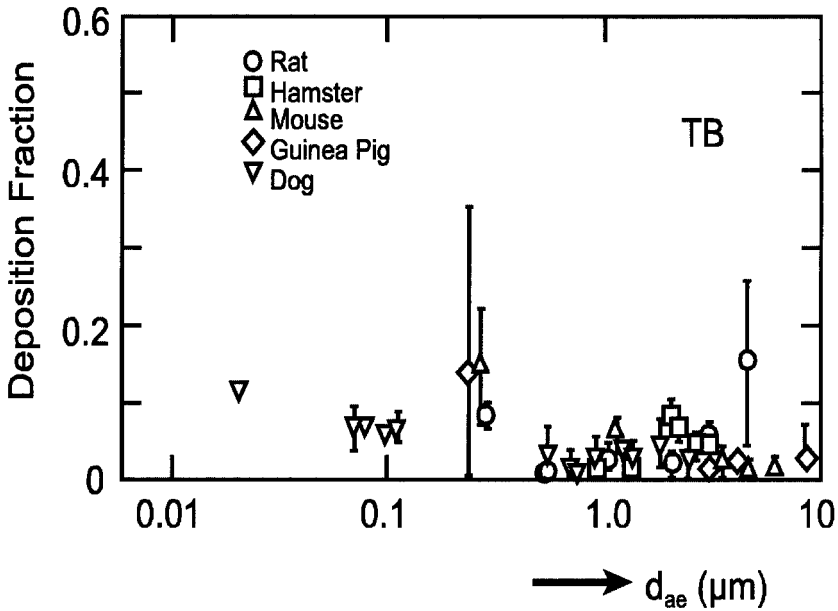


FIGURE 10. Tracheobronchial deposition fractions in various animal species as a function of particle aerodynamic diameter; for less than $0.5 \mu\text{m}$, geometric diameters were used.

Alveolar deposition in laboratory animals is depicted in Figure 12. In general, for most d_{ae} , alveolar deposition fractions in rodents are considerably lower than they are for humans. This observation has often been used by toxicologists to justify the use of exposure levels in animal inhalation studies of carcinogenicity that are many orders of magnitude greater than those likely to be encountered by humans. While this approach may be more defensible for PSP, the use of such high exposures for PSP has led to the phenomenon of “lung overload” in carcinogenicity studies for particles such as carbon black, coal, diesel soot, talc, and titanium dioxide.

SPECIES-SPECIFIC FACTORS INFLUENCING DOSIMETRY

While species-specific structures of the various respiratory tract regions in combination with the route and depth of breathing are critically important for determining where particles will deposit, there are several other factors that affect dosimetry to differing degrees in laboratory rodents and humans. Among these factors are inhalability, oronasal breathing, and heterogeneity in acinar deposition of particles. In addition, there may be morphometric differences in alveolar parameters that influence the choice of an appropriate dose metric in the lung overload scenario. These topics are briefly discussed next.

Inhalability

Laboratory animals and humans inhale particles from the air space proximal to the nares, and humans may also inhale particles from air

proximal to the mouth. The air space around these orifices is considered to be the breathing zone. The penetration of the particles into the breathing zone is influenced by airflow velocity and direction in close proximity to a person's or animal's head and body. Inhalability can be defined as the probability that a particle of a given size will actually enter one of the respiratory-tract orifices in the case of humans or enter the nares in the case of laboratory rodents, since these animals are obligatory nose breathers. Using this probability, one can adjust the concentration of particles external to the human or animal to obtain the concentration of particles in the inspired air.

Since inhalability of particles varies between species (Ménache et al., 1995), adjustments for inhalability must be made when making interspecies comparisons of exposure scenarios that lead to the same internally deposited dose. Inhalability in humans is not a factor for PSP studied thus far in animals, since the particle size range of the aerosol does not exceed $5 \mu\text{m } d_{ae}$, and since particles $<5 \mu\text{m } d_{ae}$ are completely inhalable by humans.

Using the experimental data of Raabe et al. (1988), Ménache and colleagues (1995) determined that a logistic curve adequately described the probability that laboratory rodents would inhale particles of any given size. Even for particles as small as $1 \mu\text{m } d_{ae}$, rats inhale only 93% of parti-

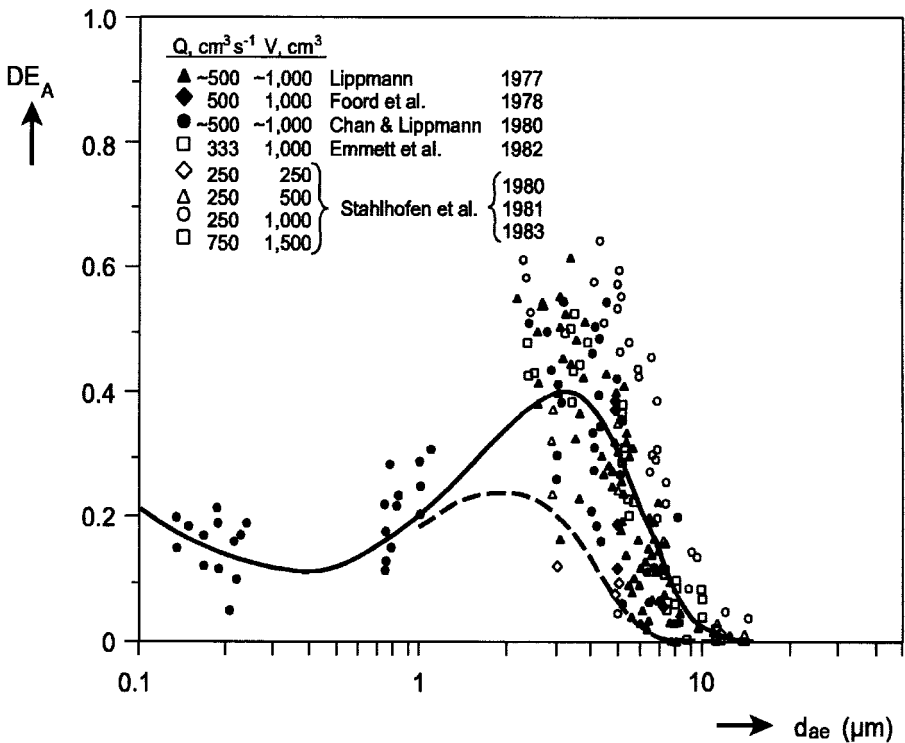


FIGURE 11. Alveolar deposition data in humans as a function of particle aerodynamic diameter (d_{ae}). The solid curve represents the mean of all the data; the broken curve is an estimate of deposition for nose breathing by Lippmann (1977). Data are from Stahlhofen et al. (1989).

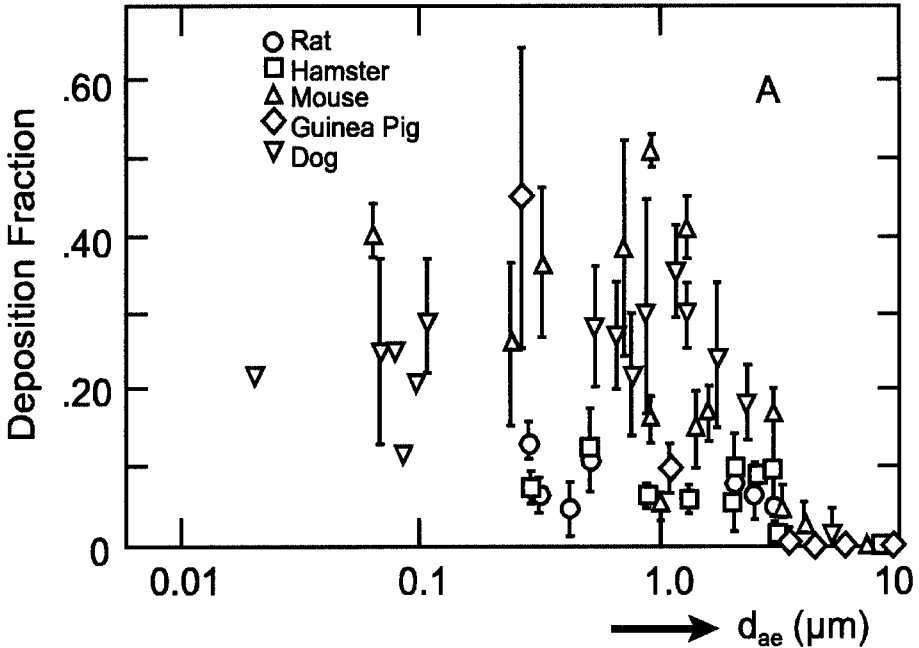


FIGURE 12. Alveolar deposition in various animal species as a function of particle aerodynamic diameter. For $<0.5 \mu\text{m}$, geometric diameters were used. Data are from Schlesinger (1988).

cles this size. Inhalability declines with increasing particle size such that 85%, 77%, 71%, and 65% of 2, 3, 4, and 5 μm d_{ae} particles, respectively, are inhaled by laboratory rodents. Independent of any difference between rats and humans in the clearance of particles, suppose one wanted to know what level humans would have to be exposed to get the same mass of particles per unit surface area deposited in the alveolar region if rats were exposed for 1 h to 5 mg/m^3 of a monodisperse aerosol of 2 μm d_{ae} particles. Using fractional alveolar deposition data for humans and rats, the inhalability equation for rodents developed by Ménache et al. (1995), pulmonary function data specific to each species, and computational procedures described by Miller et al. (1995), one finds that humans exposed for 1 h to 1.85 mg/m^3 of this aerosol would have the same mass deposited per unit surface area in the alveolar region as would rats. This computation is of course more complex for polydisperse aerosols.

Oronasal Breathing

While laboratory rodents are obligatory nose breathers, humans can breathe through either their nose or mouth. For most of the human population, individuals breathe through their nose while at rest. As ventilatory drive increases with work or exercise, humans switch to oronasal breathing when minute ventilation exceeds about 35 L min^{-1} (Niinimaa et al.,

1981). The proportion of inhaled air entering through the mouth continues to increase as minute ventilation increases beyond the oronasal switching point. Niinimaa and colleagues (1981) found, however, that 15% of subjects breathe through the mouth even at rest. Since oronasal breathing modifies the amount and the pattern of particle deposition, the activity pattern of the human subpopulation being exposed to particles of concern needs to be taken into account. Deposition equations and regional respiratory tract deposition curves that incorporate oronasal breathing have been developed by Miller et al. (1988).

Heterogeneity in Acinar Deposition

Lung overload involves an inhibition or stasis of alveolar macrophage-mediated clearance of particles. Thus, alveolar region deposition is of most concern relative to lung overload, since clearance from this region is slow. To date, experimental particulate studies for the most part have only provided information on particle deposition aggregated over large regions of the lung. In addition, nonempirical dosimetry models for particle deposition have largely been based upon typical path, whole-lung geometry models for humans (Gerrity et al., 1979; Yeh & Schum, 1980; Yu & Diu, 1983; Egan & Nixon, 1989; International Commission on Radiological Protection, 1994) as well as for rats (Schum & Yeh, 1980; Xu & Yu, 1987; Martonen et al., 1992).

The rat lung has over 2400 acini, and there is significant variability in TB path length to reach these acini (Yeh et al., 1979). Recently, Anjilvel and Asgharian (1995) developed a multiple-path model for the TB region of the rat and used this model to determine particle deposition in each acinus of the lung as a function of particle size. They studied various particle sizes and found that heterogeneity among acini in particle deposition is greatest when particles are relatively small ($\leq 0.1 \mu\text{m}$). Even for particles in the range of 2 to 3 μm d_{ae} , there is considerable variability in particle deposition among acini in the rat lung, with about 100 acini and 50 acini having deposition fractions about 25% and 50% greater, respectively, than what the average acinar deposition fraction is.

This potential for greatly enhanced deposition in some localized areas of the rat lung, coupled with the fact that rat AMs have anywhere from 82 to 145% greater volume than AMs from mice or hamsters (Table 3), may provide some insights about the lung overload phenomenon. If mouse, hamster, and rat AMs do not differ in the rate at which they can phagocytize particles, then achieving an ingested particle volume of 60% of the cell's volume, which Morrow (1988) postulated as leading to macrophage stasis, would require a longer period of exposure in rats than in mice or hamsters, given comparable deposition efficiencies among these species. Eventual macrophage death in the rat would lead to a greater lung burden of particles than in the mouse or hamster, thereby leading to a greater

TABLE 3. Interspecies comparisons of number of alveoli and of alveolar macrophage (AM) morphometric data

	Number of alveoli	Number of AM	Number of AM/ alveolus	Epithelial surface area per AM (μm^2)	AM volume (μm^3)
Mouse	4.2×10^6	2.9×10^6	0.7	17,200	493
Hamster	6.9×10^6	10.5×10^6	1.5	20,400	534
F344 rat	18.4×10^6	29.1×10^6	1.6	14,100	882
Sprague-Dawley rat	19.7×10^6	26.9×10^6	1.4	14,900	1161
Human	486×10^6	5990×10^6	12.3	17,100	1474

^aData for number of alveoli are from Mercer et al. (1994a) or derived from allometric relationships given by these authors. All other data are taken or derived from data in Stone et al. (1992), except the AM volume for F344 rat is the average of values reported by Barry et al. (1985), Chang et al. (1986), Stone et al. (1992), and Mercer et al. (1995), and the AM volume for the Sprague-Dawley rat is the average of values reported by Crapo et al. (1978) and Stone et al. (1992).

influx of macrophages and an increased likelihood of a cascade of inflammatory processes. In addition, the ability of particles to accumulate in the interstitium would be greater in rats compared to mice or hamsters. All of this suggests that a wide variety of dose metrics as well as biological factors may need to be examined in order to understand the basis for species differences that may be involved in lung overload. To that end, Table 4 presents human to rat ratios for various dose metrics as a function of particle size.

MECHANISMS OF CLEARANCE AND TRANSLOCATION

Once particles have deposited on airway surfaces, they are cleared or translocated to other sites either within the respiratory tract or external to

TABLE 4. Human to rat ratios for various alveolar region dose metrics

Diameter (μm)	Mass		Number of particles per			
	Total	Per unit area	Unit area	Ventilatory unit	Alveolus	Macrophage
0.2	53	0.14	0.14	3.88	2.15	0.27
0.4	62	0.17	0.16	4.56	2.52	0.32
0.6	72	0.19	0.19	5.30	2.93	0.37
0.8	82	0.22	0.21	6.06	3.35	0.42
1	92	0.25	0.23	6.77	3.74	0.47
2	137	0.37	0.31	10.05	5.55	0.69
3	223	0.60	0.47	16.37	9.05	1.13
4	487	1.31	0.93	35.67	19.71	2.46
5	1197	3.23	2.09	87.81	48.52	6.06

Note. Assuming monodisperse particles of unit density and adjusting for inhalability in the rat.

it. The mechanisms that are operative for clearance and translocation of particles differ among the extrathoracic, tracheobronchial, and alveolar regions. Since this review is concerned with PSP, dissolution processes will not be considered. That is, for particles exerting their toxicity or carcinogenicity through the phenomenon of lung overload, the rate of clearance by dissolution is insignificant compared to the rate of clearance of the intact particles. In addition, while we considered ET deposition in order to illustrate the filtering effect of this region on particles being available to deposit in the TB and A regions, ET clearance and translocation mechanisms do not need to be discussed relative to lung overload.

TB Region Clearance

For PSP, the primary mechanism for clearance from the TB region is via the mucociliary escalator. The mucous layer lining the conducting airways is continually propelled cephalad by the beating of cilia until reaching the oropharynx, where the fluid is swallowed. In large airways, deposited particles tend to move in a spiral fashion on the mucous layer from the site of initial deposition until reaching the dorsal surface, after which they proceed longitudinally along this surface to the larynx (Wolff & Muggenburg, 1979). The nature of particle movement on the mucociliary escalator has not been examined in small airways. As noted earlier, the thickness of the mucous layer varies by location. While some investigators have reported that the mucous layer is not continuous, others have reported it to be continuous (Table 2). Regardless, there is general agreement that some regions within airway bifurcations have areas of nonciliated cells, leading to retarded clearance of particles from these areas. Interestingly, as noted earlier, airway bifurcations have been shown to be hot spots for particle deposition due to enhanced impaction losses at these sites during inspiration.

Clearance of particles from the trachea and large TB airways can be facilitated in humans by coughing. While a minor mechanism for clearance in healthy subjects, cough can be very important in individuals with severe respiratory disease, where coughing serves to dislodge mucus and other deposited material from the surfaces of larger airways. Another potential mechanism for TB clearance of PSP is through phagocytosis of particles by macrophages resident in the conducting airways. Gehr and colleagues (1990) have shown that particles initially deposited in conducting airways can be found retained in the airways in close association with the epithelium and that such particles are coated with an osmiophilic film attributable to surfactant. Particles retained in close proximity to the epithelium would tend to remain there until engulfed by resident macrophages.

Alveolar Region Clearance

As can be seen from Figure 13, there are a number of mechanisms and pathways that can be important for the clearance or translocation of

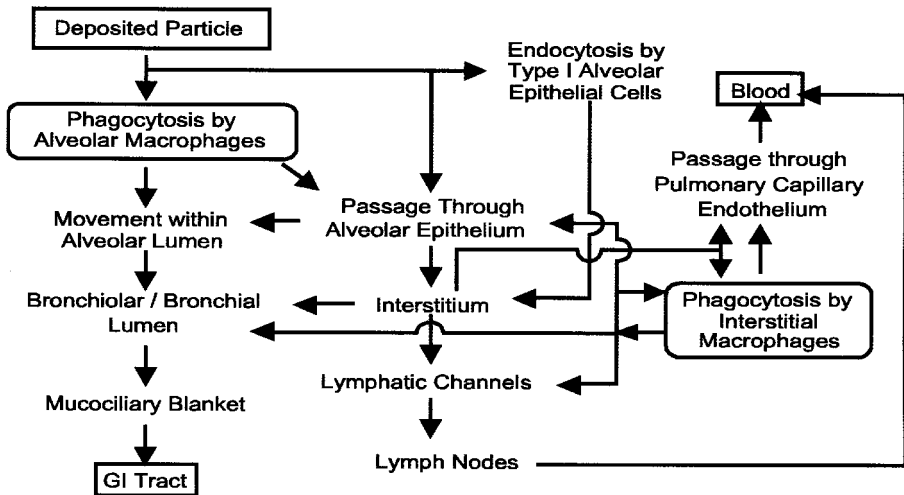


FIGURE 13. Schematic of known and suspected clearance pathways for poorly soluble particles depositing in the alveolar region. Modified from U.S. Environmental Protection Agency (1996).

particles from the alveolar region. Which mechanisms and pathways are operative at any point in time is a complex function of exposure rate and level, particle size, particle number, and current mass load. The same pathways for clearance of particles appear to be operative in laboratory animals and humans, although the relative importance of the various pathways appears to vary considerably among species (Snipes, 1989).

Alveolar macrophage phagocytosis of deposited particles is clearly the predominant clearance process for the alveolar region. Macrophages reside on the epithelium and come into contact with particles through either random motion or chemotactic factors (Warheit et al. 1988). Chemotaxis may not be requisite for phagocytosis of particles by macrophages, since Hadley (1977) calculated that a single rat AM can scavenge about 35% of an alveolus of this species using "agrapod-like" extensions of its cell membrane. Despite tremendous differences in lung size, number of alveoli, and number of AMs between laboratory rodents and humans, the amount of epithelial surface area per AM is amazingly similar across these species (Table 3).

Translocation from the alveolar region of particles that have been ingested by macrophages primarily occurs by one of two pathways: (1) the mucociliary escalator, or (2) via pathways to the lung-associated lymph nodes (LALN). As can be seen from Figure 13, the pathways leading to particles ending up in LALN are relatively tortuous compared to translocation of particles via the mucociliary escalator.

Some of the particles passing through the alveolar epithelium and into the interstitium escape phagocytosis by interstitial macrophages. These particles contribute to the interstitial load and can move to various sites

(perivenous, peribronchiolar, lymphatics, subpleural) before becoming trapped and increasing lung particle burdens. Accumulation of particles in interstitial spaces with chronic exposure to high levels of poorly soluble particles is a hallmark of the lung overload phenomenon (Morrow, 1994). Uningested particles in the interstitium may also pass through the capillary endothelium and directly enter the blood stream (Raabe, 1982).

CLEARANCE KINETICS

The potential for inhaled particles to exert toxic or carcinogenic effects is greatly influenced by their residence time at target sites. Residence time is particularly important for rodent inhalation studies using PSP, since particle-tissue contact is not diminished much by dissolution of the particles during the short life span of rodents. Clearance kinetics are influenced by a number of factors such as the inhaled particle size distribution, the respiratory pattern used, and the respiratory-tract anatomy of the species being studied (Wolff, 1992). As a result, there are significant differences among species in rates of clearance of inhaled particles from the ET, TB, and A regions. Since clearance time of particles from various parts of the ET region is typically less than 30 min, the clearance kinetics for this region are of little relevance to issues of lung overload and are not discussed here. The net result of these species and regional differences presents a clear challenge to toxicologists and risk assessors for interpreting results from animal studies as to their relevance to humans.

TB Region Clearance Kinetics

Mucous velocities and hence the transport of particles vary considerably (Table 2) in different-sized TB airways. This variability is over and above the variability imparted by the use of various experimental methods to assess clearance rates in laboratory animals and humans (Schlesinger, 1985). Interindividual variability can largely be overcome by the use of radiolabeled particles and repeated measurements being made on the same subject or animal, since highly reproducible results are usually obtained for any given subject or animal. For the percent of particles depositing in the TB region, 90% of relatively insoluble particles are cleared within 2.5–20 h (Albert et al., 1973), while bronchial clearance is about 99% complete by 48 h after exposure (Bailey et al., 1985). Individual subject geometry of the conducting airways and particle size are important sources of variability in measurements of TB clearance rates.

Some aspects of TB clearance remain controversial. Among these are conflicting interpretations concerning the reason why a small fraction (about 1%) of PSP appear to be retained for a long time (Gore & Patrick, 1982) compared to other investigators finding that up to 40% of particles likely to have been deposited in conducting airways are not cleared for days and that this effect is inversely related to particle size (Stahlhofen et

al., 1986). A surfactant film on the mucous layer, enhanced deposition at bifurcations and correspondingly low clearance from these areas, as well as heterogeneity in TB path length and the presence of airway macrophages, have been postulated as potential explanations.

Alveolar Region Clearance Kinetics

In general, clearance of PSP from the alveolar region consists of two phases. The first phase is typically measured in days, while the slower second phase occurs over a period of months to years. In addition to variability imparted by the use of different techniques, the physicochemical properties of the particle are important determinants of alveolar region clearance kinetics. A particularly important observation for particles for which lung overload has been shown to be operative is the fact that once any dissolution has been accounted for, mechanical removal by AMs via the mucociliary escalator or the lymphatics appears to be independent of size for particles $<5 \mu\text{m } d_{ae}$ (Snipes et al., 1983). This finding justifies the synthesis of results from a wide variety of particle types and sizes when considering lung overload issues. However, given the wide range of clearance rates of identical particles among human subjects (Bailey et al., 1985), chronic exposures will have associated with them large variations in alveolar region particle burdens, thereby leading to significant uncertainties about comparable exposure scenarios between laboratory rodents and humans. In addition, since rats have more rapid alveolar clearance kinetics than do humans (Snipes, 1989), the difficulty in identifying equivalent exposure scenarios leading to lung overload in these two species is compounded but approachable through the development of dosimetry models.

While overall alveolar region clearance kinetics have been studied, data on clearance kinetics along the various clearance pathways depicted in Figure 13 are scant. Uningested particles can penetrate into the interstitium via endocytosis of Type 1 epithelial cells in a matter of hours following deposition (Brody et al., 1981). This pathway has been shown to be increasingly important as particle loading increases and appears to be even more important when particle levels exceed the saturation point for increasing macrophage number (Adamson & Bowden, 1978).

Clearance kinetics via the lymphatic system appear to be temporally dependent upon effectiveness (or lack thereof) of other clearance pathways. Greenspan and colleagues (1988) showed that when the phagocytic activity of macrophages decreases, lymphatic translocation tends to increase, such as would be the case for lung overload. Lymphatic translocation rates appear to be particle size dependent in rats for particles in the aerodynamic size range, with smaller particles translocating faster than larger ones (Snipes & Clem, 1981; Takahashi et al., 1992). Although comparable data are lacking for humans, similar relationships likely hold also in people. Translocation rates to the lymphatic system are on the order of

0.02–0.003%/day (Snipes, 1989), with elimination from the lymph nodes occurring over half-times likely to be in the tens of years (Roy, 1989).

LUNG OVERLOAD

Since Morrow (1988) reviewed the evidence for dust overloading of the lungs and postulated that the phenomenon reflected a breakdown of AM-mediated clearance of PSP induced by a volumetric overload, additional experimental studies and insights about lung overload have led to a better characterization of general aspects of pulmonary responses during overload. These aspects include: (1) stasis or slowing of AM-mediated clearance of PSP, (2) significant and diverse accumulation of PSP-laden AMs within pulmonary alveoli, (3) increased translocation and accumulation of PSP in the interstitium of the lung and in the lymph nodes of the thoracic cavity, (4) chronic inflammation in the lung, (5) the eventual appearance of alveolitis and granulomatous lung disease, and (6) the potential development of lung tumors (Snipes, 1995). Interestingly, despite evidence that studies in mice and hamsters have achieved lung burdens that are considered to be in the overload range, only rats have developed lung tumors, with no study of PSP having identified lung tumors at a nonoverload exposure level. This has led to the question of the relevance of PSP-associated lung tumors for assessing potential carcinogenic risk to humans.

Although one of the hallmarks of lung overload is stasis or significant slowing of AM-mediated clearance of PSP, there is not necessarily a decrease in phagocytic activity of AMs (Morrow, 1992). In fact, Morrow's (1992) analysis of the results of the particle clearance studies of Bellmann et al. (1991) led him to conclude that phagocytosis is a fast process relative to clearance and that phagocytosis by immobilized macrophages must continue to occur. Earlier, Morrow (1988) had hypothesized that volumetric loading of AMs was the driving function leading to the loss of mobility of these cells, with a threshold for the start of overload being 6% of the volume of an AM and with stasis occurring at a 60% volumetric loading level. With a more definitive and broader array of lung morphometric data being available now for laboratory rodents and humans (Stone et al., 1992), some interesting comparisons among species become apparent relative to the potential for volumetric loading of particles by AM of various species (Table 5). After accounting for the volume of the AM nucleus and the void space volume (Stöber, 1972), one sees that only about 90 to 120 uniform, 1.9- μm particles would need to be engulfed to exceed the volume for overload in rats, rather than about 150 such particles as Morrow (1988) computed. Such substantially lower numbers, as found in Table 5, for volumetric particle overload support the recent modeling work of Stöber and colleagues (1998), indicating that the initiation of lung overload may occur at considerably lower exposure levels

than previously believed required (i.e., in the range of 150–200 $\mu\text{g}/\text{m}^3$). Currently, however, there are no experimental data that can be used to confirm or refute these modeling predictions. Table 5 shows that essentially phagocytosis of a single 10- μm particle is sufficient to induce stasis of AM in rodents and in humans. Interestingly, Oberdörster et al. (1992) showed that F344 rats can engulf such particles but do not appreciably transport them from the lungs.

While the data in Table 5 give one some idea about the number of engulfed particles leading to stasis in various rodent and human AMs as a function of particle size, the time scale over which stasis might occur depends upon species ventilatory patterns and alveolar region morphometric parameters, the level and duration of exposure, and the rates of deposition and clearance of particles. If one ignores clearance, dosimetry calculations are available from Miller et al. (1995) that can be used together with the data of Table 5 to predict the earliest times at which stasis might occur for various exposure scenarios. Suppose, for example, that F344 rats and humans were exposed 24 h/day to 10 mg/m^3 of aerosols of 1- μm or 5- μm particles. For 1- μm particles, about 80 days of exposure would yield stasis of AM in rats, compared to about 310 days in humans. And for 5- μm particles, the corresponding numbers would be about 300 and 90 days, respectively. The fact that lung overload has been observed much later than these times in rodents exposed chronically to 10 mg/m^3 of PSP reflects the importance of clearance as a mechanism to reduce body burdens.

The strong inverse linear relationship ($r^2 = .98$) between the clearance of PSP from the lung and the volume of such particles in the lung is depicted in Figure 14. Morrow (1994) suggests that the mass concentrations in the lung leading to the onset of reduced AM clearance and eventual stasis of 1 and 10 mg/g of lung, respectively, should be expressed in terms of the volumetric inhibition of AM mobility. This leads to 1,000 and 10,000 nl/g lung, respectively, as the dust loadings in Figure 14 associated with the onset and eventual stasis of AM mobility. The strength of the relationship between the pulmonary clearance coefficient, k , and the volume of dust in the lung from data pooled across studies in rats that used differing exposure levels of various types of PSP lends strong support to volumetric inhibition of AM as being a unifying concept for the basis of lung overload.

However, data such as contained in Figure 14 do not provide insights as to the biological mechanisms involved, the relative importance of the various alveolar region clearance pathways (Figure 13), temporal shifts in clearance pathways, or the dose metrics that may be more proximally associated with critical steps in the process of lung overload. Relative to dose metrics, Driscoll (1996) found a strong correlation between the percent of rats with lung tumors in various PSP studies and the lung burden expressed as the surface area of the particles in square meters per lung.

TABLE 5. Alveolar macrophage morphometric data in relationship to volumetric particle overload

	Volume of		Volume for cell stasis ^c (μm^3)	Number of engulfed particles leading to stasis ^d										
	Cell ^a (μm^3)	Nucleus ^b (μm^3)		0.1 μm	0.5 μm	1 μm	1.5 μm	2 μm	2.5 μm	3 μm	3.5 μm	4 μm	5 μm	10 μm
Mouse	493	124	221	304,423	2435	304	90	38	19	11	7	5	2	0.30
Hamster	534	117	250	344,022	2752	344	102	43	22	13	8	5	3	0.34
F344 rat	882	121	456	627,407	5019	627	186	78	40	23	15	10	5	0.63
Sprague-Dawley rat	1161	153	605	831,181	6649	831	246	104	53	31	19	13	7	0.83
Human	1474	121	812	1,116,216	8930	1116	331	140	71	41	26	17	9	1.12

^aData for the mouse, hamster, and human are from Stone et al. (1992). Value for the F344 rat is average of Stone et al. (1992), Barry et al. (1985), Chang et al. (1986), and Mercer et al. (1995). Value for the Sprague-Dawley rat is average of Stone et al. (1992) and Cirapo et al. (1978).

^bData are from Table 4 in Stone et al. (1992). The mean value of 121 μm^3 was assigned to F344 rats and humans since Stone et al. did not give values for these species.

^cVolume taking into account the volume of the cell's nucleus.

^dIncludes adjusting for the void space volume (Stöber, 1972) created by the packing of uniform spheres.

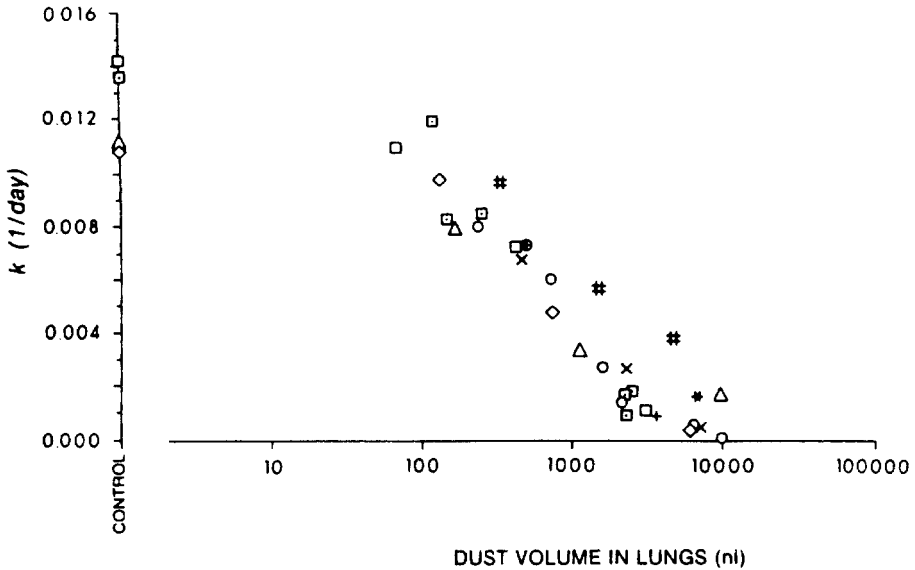


FIGURE 14. The pulmonary clearance coefficient, k , is correlated with the retained pulmonary dust volume (nl) and progressively decreases as the particulate volume increases. Data are from the studies indicated: (□) toner, Bellmann et al. (1989); (○) toner, Muhle et al. (1990b); (□, ◇, △) toner, Muhle et al. (1988, 1991); (+, ⊕) titanium dioxide, Muhle et al. (1988, 1990c); (X) diesel, Heinrich et al. (1986, 1989); (#) polyvinyl chloride, Muhle et al. (1990a); (*) carbon black, Muhle et al. (1990c). From Morrow (1994).

Driscoll (1996) only used the dose levels that yielded statistically significant increases in tumors in his correlation analysis. For Figure 15, Driscoll's surface-area data were used but the tumor data were expressed as the fraction of rats with lung tumors. A logistic curve fit using all data points still demonstrates a strong relationship between the fraction of rats having lung tumors as a function of the surface area of particles per lung. Collectively, the data shown in Figures 14 and 15 establish three principles that are critically important for the carcinogenic risk assessment of PSP: (1) Substantial lung overload is requisite for induction of lung tumors in rodents, (2) some of the biological mechanisms involved with lung overload are likely not operative at nonoverload exposure levels, and (3) a critical retained lung burden must exist for any given PSP such that exposure levels depicted schematically by curves A and B of Figure 1 can be identified and for which there is essentially no carcinogenic risk.

Given the complex relationships between deposition mechanisms, clearance pathways and kinetics, and morphometric characteristics of various alveolar parameters, the most reasonable path forward in understanding lung overload and establishing critical lung burdens associated with this phenomenon must involve the use of physiologically based dosimetry models. Physiologically based dosimetry models can incorporate the nec-

essary complexities and help identify experimental studies that will shed light on the issues needing resolution and that will enable important model parameters to be estimated. Stöber and colleagues (1989, 1990a, 1990b, 1994) have developed various physiologically based dosimetry models and have used them to advance our understanding of key aspects of lung overload. For example, Stöber and Mauderly (1994) used such a model to examine the hypothesis that the time integral of the interstitial burden can be used as an effective relative dose for overload carcinogenesis in the rat. They incorporated new data on temporal patterns of lymph-node burdens of PSP and were able to obtain reasonable fits to the experimental data by adjusting interstitial clearance kinetics. Given the variability in the experimental data, Stöber and Mauderly (1994) categorized their efforts as leading to dose-response interpretations that were better founded on a theoretical basis but that might still be considered as speculative. Nonetheless, while one might have to agree with Morrow (1994) that currently we are only able to speculate on the relative roles of the complex mechanisms and factors leading to lung overload, dosimetry and biologically based dose-response modeling will undoubtedly be needed to synthesize our knowledge about lung overload and to identify critical data gaps. For an in-depth review of recent progress in using physiologically based dosimetry to examine the retention and clearance of PSP, the reader is referred to Stöber and McClellan (1997).

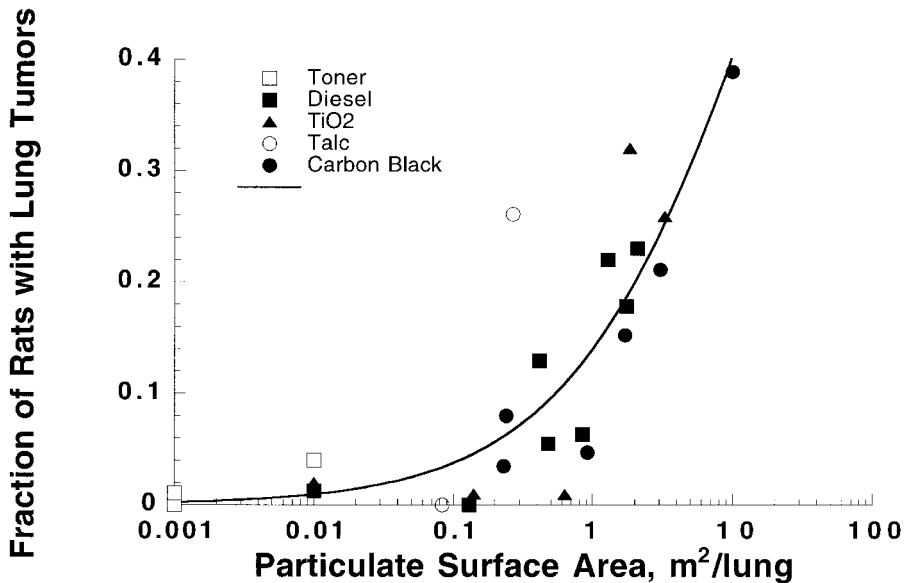


FIGURE 15. Fraction of rats with lung tumors after exposure to various PSPs as a function of the particulate surface area in the lung. The figure is based on data contained in Driscoll (1996). The solid curve represents the fit of a logistic function of the form $y = [1 + e^{-(\alpha + \beta \log x)}]^{-1}$, where y represents the fraction of rats with lung tumors, and x represents the surface area of the particles in the lung. The fitted values of the parameters α and β are -1.828 and 1.419 , respectively; here $R^2 = .71$.

SUMMARY

Despite significant structural differences between laboratory animals and humans in various regions of the respiratory tract, the same major mechanisms of deposition are operative for poorly soluble particles, although the relative importance of these mechanisms in a given region may also differ between laboratory animals and humans. For particles $< 0.5 \mu\text{m}$ in size, the geometric diameter is the key physical property important for deposition, while for particles $> 0.5 \mu\text{m}$, the aerodynamic equivalent diameter of the particle is an important aspect of deposition mechanisms since it takes into account the size, shape, and density of the particle.

Complex interactions among species-specific respiratory tract anatomy, the route and depth of breathing, and particle-specific physical properties determine the sites of deposition of particles at various locations with the respiratory tract. These interactions also impart significant intersubject variability in experimental studies on the regional respiratory tract deposition of PSP in human subjects. Considerably more particulate deposition data are available for humans than for laboratory animals.

Most PSP that are of concern are less than $5 \mu\text{m } d_{ae}$ and are completely inhalable by humans; however, such is not the case for rodents. The significantly decreased probability of rodents being able to inhale PSP must be taken into account when estimating exposure scenarios that would be expected to lead to comparable deposits of PSP at specific target sites in the lungs of rodents and humans. Such comparisons are further complicated if the human activity pattern of interest includes ventilation levels that result in humans switching to oronasal breathing, since the oral pathway is less efficient than the nasal pathway at removing particles and so the thoracic burden of particles is increased.

Once PSP are deposited, the mechanisms available for the clearance and translocation of PSP vary among the major respiratory tract regions (ET, TB, and A). The specific mechanisms and pathways that are operative at any particular point in time are a complex function of exposure rate and level, particle size, particle number, and current mass loading. While the same pathways for clearance of particles in laboratory animals also appear to be operative in humans, the relative importance of these pathways can vary considerably among animals and humans. Importantly, once any dissolution of particles has been accounted for, mechanical removal by AMs via the mucociliary escalator or the lymphatics is essentially independent of size for particles $< 5 \mu\text{m } d_{ae}$. Thus, results from a wide variety of PSP types and sizes can collectively be used to examine the phenomenon of lung overload.

Relative to issues associated with lung overload, the impairment of alveolar macrophage-mediated clearance of PSP is central. The strength of the inverse linear relationship between the pulmonary clearance coef-

ficient and the volume of dust in the lung from data pooled across studies in rats that used different exposure levels of various types of PSP lends strong support to volumetric inhibition of AM as being a unifying concept for the basis of lung overload. Tumors resulting from exposure to high levels of PSP are alveolar in origin. To date, such tumors have only been observed in rats, despite evidence that mice and hamsters have also been exposed to sufficiently high levels of PSP so as to induce lung overload. Given that rat AMs can have about twice the volume of mouse or hamster AMs and that inhibition of macrophage-mediated particle clearance appears necessary for the development of lung overload, examining various AM-based dose metrics may aid in understanding the basis for species differences involved in lung overload.

Given the complex relationships between deposition mechanisms, clearance pathways and kinetics, and morphometric characteristics of various alveolar region parameters, physiologically based dosimetry models offer the best opportunity to synthesize our current knowledge of lung overload and to identify critical data gaps that prevent the resolution of issues surrounding this phenomenon. Substantial lung overload is requisite for induction of lung tumors in rats, and some of the biological mechanisms involved in lung overload are likely not operative at nonoverload exposure levels. Thus, a critical retained lung burden should exist for any given PSP for which there is no carcinogenic risk. Determining that critical retained lung burden in a laboratory animal and extrapolating that result to humans is difficult at best and is likely impossible without the use of physiologically based modeling.

REFERENCES

- Adamson, I. Y. R., and Bowden, D. H. 1978. Adaptive responses of the pulmonary macrophagic system to carbon: II. Morphologic studies. *Lab. Invest.* 38:430-438.
- Albert, R. E., Lippmann, M., Peterson, H. T., Jr., Berger, J., Sanborn, K., and Bohning, D. 1973. Bronchial deposition and clearance of aerosols. *Arch. Intern. Med.* 131:115-127.
- Andersen, I., Lundqvist, G. R., and Proctor, D. F. 1971. Human nasal mucosal function in a controlled climate. *Arch. Environ. Health* 23:408-420.
- Anjilvel, S., and Asgharian, B. 1995. A multiple-path model of particle deposition in the rat lung. *Fundam. Appl. Toxicol.* 28:41-50.
- Bailey, M. R., Hodgson, A., and Smith, H. 1985. Respiratory tract retention of relatively insoluble particles in rodents. *J. Aerosol Sci.* 16:295-305.
- Barry, B. E., Miller, F. J., and Crapo, J. D. 1985. Effects of inhalation of 0.12 and 0.25 parts per million ozone on the proximal alveolar region of juvenile and adult rats. *Lab. Invest.* 53:692-704.
- Bellmann, B., Muhle, H., Creutzenberg, O., Kilpper, R., Morrow, R., and Mermelstein, R. 1989. Reversibility of clearance impairment after subchronic test toner inhalation. *Exp. Pathol.* 37:234-238.
- Bellmann, B., Muhle, H., Creutzenberg, O., Dasenbrock, C., Kilpper, R., MacKenzie, J. C., Morrow, P., and Mermelstein, R. 1991. Lung clearance and retention of toner, utilizing a tracer technique during a long-term inhalation study in rats. *Fundam. Appl. Toxicol.* 17:300-313.
- Brody, A. R., Hill, L. H., Adkins, B., Jr., and O'Connor, R. W. 1981. Chrysotile asbestos inhalation in rats: Deposition pattern and reaction of alveolar epithelium and pulmonary macrophages. *Am. Rev. Respir. Dis.* 123:670-679.

- Chan, T. L., and Lippmann, M. 1980. Experimental measurements and empirical modelling of the regional deposition of inhaled particles in humans. *Am. Ind. Hyg. Assoc. J.* 41:399–409.
- Chang, L. Y., Graham, J. A., Miller, F. J., Ospital, J. J., and Crapo, J. D. 1986. Effects of subchronic inhalation of low levels of nitrogen dioxide. 1. The proximal alveolar region of juvenile and adult rats. *Toxicol. Appl. Pharmacol.* 83:45–61.
- Cohen, B. S. 1987. Deposition of ultrafine particles in the human tracheobronchial tree: A determinant of the dose from radon daughters. In *Radon and its decay products*, ed. P. H. Hopke, pp. 475–486. Washington, DC: American Chemical Society.
- Cohen, B. S., Susman, R. G., and Lippmann, M. 1990. Ultrafine deposition in a human tracheobronchial cast. *Aerosol Sci. Technol.* 12:1082–1091.
- Crapo, J. D., Peters-Golden, M., Marsh-Salin, J., and Shelburne, J. S. 1978. Pathologic changes in the lungs of oxygen-adapted rats: A morphometric analysis. *Lab. Invest.* 39:640–653.
- Crapo, J. D., Chang, Y. L., Miller, F. J., and Mercer, R. R. 1990. Aspects of respiratory tract structure and function important for dosimetry modeling: Interspecies comparisons. In *Principles of route-to-route extrapolation for risk assessment*, eds. J. R. Gerrity and C. J. Henry, pp. 15–32. New York: Elsevier.
- Dahl, A. R., Bice, D. E., Hahn, F. F., Henderson, R. F., Mauderly, J. L., Muggenburg, B. A., Pickrell, J. A., Wolff, R. K., and Hobbs, C. H. 1986. Acute and Subchronic Toxicity of Methylphosphoric Difluoride (DF) by Inhalation in Rats. Aberdeen Proving Ground, MD: U.S. Army Chemical Research and Development Center.
- Davidson, M. R., and Fitz-Gerald, J. M. 1974. Transport of O₂ along a model pathway through the respiratory region of the lung. *Bull. Math. Biol.* 36:275–303.
- Driscoll, K. E. 1996. Role of inflammation in the development of rat lung tumors in response to chronic particle exposure. *Inhal. Toxicol.* 8(suppl.):139–153.
- Egan, M. J., and Nixon, W. 1989. On the relationship between experimental data for total deposition and model calculations—Part II: Application to fine particle deposition in the respiratory tract. *J. Aerosol Sci.* 20:149–156.
- Emmett, P. C., Aitken, R. J., and Hannan, W. J. 1982. Measurements of the total and regional deposition of inhaled particles in the human respiratory tract. *J. Aerosol Sci.* 13:549–560.
- Felicetti, S. A., Wolff, R. K., and Muggenburg, B. A. 1981. Comparison of tracheal mucous transport in rats, guinea pigs, rabbits, and dogs. *J. Appl. Physiol.* 51:1612–1617.
- Foord, N., Black, A., and Walsh, M. 1978. Regional deposition of 2.5–7.5 μm diameter inhaled particles in healthy male non-smokers. *J. Aerosol Sci.* 9:343–357.
- Gehr, P., Schürch, S., Berthiaume, Y., Im Hof, V., and Geiser, M. 1990. Particle retention in airways by surfactant. *J. Aerosol Med.* 3:27–43.
- Gerrity, T. R., Lee, P. S., Hass, F. J., Marinelli, A., Werner, P., and Laurencio, R. V. 1979. Calculated deposition of inhaled particles in the airway generations of normal subjects. *J. Appl. Physiol. Respir. Environ. Exercise Physiol.* 47:867–873.
- Giacomelli-Maltoni, G., Melandri, C., Prodi, V., and Taroni, G. 1972. Deposition efficiency of monodisperse particles in human respiratory tract. *Am. Ind. Hyg. Assoc. J.* 33:603–610.
- Giordano, A. M., and Morrow, P. E. 1972. Chronic low-level nitrogen dioxide exposure and mucociliary clearance. *Arch. Environ. Health* 25:443–449.
- Goodman, R. M., Yergin, B. M., Landa, J. F., Golivanaux, M. H., and Sackner, M. A. 1978. Relationship of smoking history and pulmonary function tests to tracheal mucous velocity in nonsmokers, young smokers, ex-smokers, and patients with chronic bronchitis. *Am. Rev. Respir. Dis.* 117:205–214.
- Gore, D. J., and Patrick, G. A. 1982. A quantitative study of the penetration of insoluble particles into the tissue of the conducting airways. In *Inhaled particles V: Proceedings of an international symposium*, September 1980. Cardiff, Wales, ed. W. H. Walton, *Ann. Occup. Hyg.* 26:149–161.
- Greenspan, B. J., Morrow, P. E., and Ferin, J. 1988. Effects of aerosol exposures to cadmium chloride on the clearance of titanium dioxide from the lungs of rats. *Exp. Lung Res.* 14:491–499.
- Hadley, J. 1977. Membrane receptors of the alveolar macrophage: Alterations by environmental contaminants. Doctoral thesis, Duke University, Durham, NC.
- Hahn, I., Scherer, P. W., and Mozell, M. M. 1993. Velocity profiles measured for airflow through a large-scale model of the human nasal cavity. *J. Appl. Physiol.* 75:2273–2287.

- Harkema, J. R. 1992. Epithelial cells of the nasal passages. In *Comparative biology of the normal lung*, ed. R. A. Parent, pp. 27–36. Boca Raton, FL: CRC Press.
- Hatch, G. E. 1992. Comparative biochemistry of airway lining fluid. In *Comparative biology of the normal lung*, ed. R. A. Parent, pp. 617–632. Boca Raton, FL: CRC Press.
- Heinrich, U., Muhle, H., Takenaka, S., Ernst, H., Fuhst, R., Mohr, U., Pott, F., and Stöber, W. 1986. Chronic effects on the respiratory tract of hamsters, mice and rats after long-term inhalation of high concentrations of filtered and unfiltered diesel engine emissions. *J. Appl. Toxicol.* 6:383.
- Heinrich, U., Fuhst, R., Peters, L., Muhle, H., Dasenbrock, C., and Pott, F. 1989. Comparative long-term animal inhalation studies using various particulate matter objectives, experimental designs, and preliminary result. *Exp. Pathol.* 37:27.
- Horsfield, K., Dart, G., Olson, E., Filley, G. F., and Cumming, G. 1971. Models of the human bronchial tree. *J. Appl. Physiol.* 31:207–217.
- Hounam, R. F., Black, A., and Walsh, M. 1971. The deposition of aerosol particles in the nasopharyngeal region of the human respiratory tract. *J. Aerosol Sci.* 2:47–61.
- International Commission on Radiological Protection. 1994. *Human respiratory tract model for radiological protection: A report of a task group of the International Commission on Radiological Protection*. Oxford: Elsevier. ICRP publication 66. *Ann. ICRP* 24:1–3.
- Iravani, J., and van As, A. 1972. Mucus transport in the tracheobronchial tree of the normal and bronchitic rat. *J. Pathol.* 106:81–93.
- Kimbell, J. S., Gross, E. A., Joyner, D. J., Godo, M. N., and Morgan, K. T. 1993. Application of computational fluid dynamics to regional dosimetry of inhaled chemicals in the upper respiratory tract of the rat. *Toxicol. Appl. Pharmacol.* 121:253–263.
- Landahl, H. D., and Tracewell, T. 1949. Penetration of air-borne particles through the human nose II. *J. Ind. Hyg. Toxicol.* 31:55–59.
- Lippmann, M. 1970. Deposition and clearance of inhaled particles in the human nose. *Ann. Otol. Rhinol. Laryngol.* 79:519–528.
- Lippmann, M. 1977. Regional deposition of particles in the human respiratory tract. In *Handbook of physiology, section 9: Reactions to physical agents*, eds. D. H. K. Lee, H. L. Falk, S. D. Murphy, and S. R. Geiger, pp. 213–232. Bethesda, MD: American Physiological Society.
- Luchtel, D. L. 1976. Ultrastructural observations on the mucous layer in pulmonary airways. *J. Cell Biol.* 70:350a.
- Luchtel, D. L. 1978. The mucous layer of the trachea and major bronchi in the rat. *Scanning Electron Microsc.* 11:1089–1098.
- Martens, A., and Jacobi, W. 1973. Die In-vivo bestimmung der aerosolteilchen-deposition im atmen-trakt bei mund-bzw. nasenatmung. [In vivo determination of aerosol particle deposition in the total respiratory tract]. In *Aerosole in physik, medizin und technik*, pp. 117–121. Bad Soden, West Germany: Gesellschaft für Aerosolforschung.
- Martonen, T. B. 1983. On the fate of inhaled particles in the human: A comparison of experimental data with theoretical computations based on a symmetric and asymmetric lung. *Bull. Math. Biol.* 45:409–424.
- Martonen, T. B., and Hofmann, W. 1986. Factors to be considered in a dosimetry model for risk assessment of inhaled particles. *Radiat. Protect. Dosim.* 15:225–232.
- Martonen, T. B., Zhang, Z., and Yang, Y. 1992. Extrapolation modeling of aerosol deposition in human and laboratory rat lungs. *Inhal. Toxicol.* 4:303–324.
- McClellan, R. O., and Miller, F. J. 1997. An overview of EPA's proposed revision of the particulate matter standard. *CIIT Activ.* 17:1–23.
- Ménache, M. G., Miller, F. J., and Raabe, O. G. 1995. Particle inhalability curves for humans and small laboratory animals. *Ann. Occup. Hyg.* 39:317–328.
- Ménache, M. G., Raabe, O. G., and Miller, F. J. 1996. An empirical dosimetry model of aerodynamic particle deposition in the rat respiratory tract. *Inhal. Toxicol.* 8:539–578.
- Mercer, R. R., and Crapo, J. D. 1987. Three-dimensional reconstruction of the rat acinus. *J. Appl. Physiol.* 63:785–794.
- Mercer, R. R., and Crapo, J. D. 1990. Spatial distribution of collagen and elastin. *J. Appl. Physiol.* 69:756–765.

- Mercer, R. R., Russell, M. L., and Crapo, J. D. 1992. Mucous lining layers in human and rat airways. *Am. Rev. Respir. Dis.* 145:355.
- Mercer, R. R., Russell, M. L., and Crapo, J. D. 1994a. Alveolar septal structure in different species. *J. Appl. Physiol.* 77:1060–1066.
- Mercer, R. R., Russell, M. L., Roggli, V. L., and Crapo, J. D. 1994b. Cell number and distribution in human and rat airways. *Am. J. Respir. Cell Mol. Biol.* 10:613–624.
- Mercer, R. R., Costa, D. L., and Crapo, J. D. 1995. Effects of prolonged exposure to nitric oxide or nitrogen dioxide on the alveolar septa of the adult rat lung. *Lab. Invest.* 73:20–28.
- Miller, F. J., and Kimbell, J. S. 1995. Regional dosimetry of inhaled gases. In *Concepts in inhalation toxicology*, eds. R. O. McClellan and R. F. Henderson, pp. 257–287. Washington, DC: Taylor & Francis.
- Miller, F. J., Martonen, T. B., Ménache, M. G., Graham, R. C., Spektor, D. M., and Lippmann, M. 1988. Influence of breathing mode and activity level on the regional deposition of inhaled particles and implications for regulatory standards. In *Inhaled particles VI: Proceedings of an international symposium and workshop on lung dosimetry*, September 1985, Cambridge, United Kingdom, eds. J. Dodgson, R. I. McCallum, M. R. Bailey, et al. *Ann. Occup. Hyg.* 32(suppl. 1): 3–10.
- Miller, F. J., Anjilvel, S., Ménache, M. G., Asgharian, B., and Gerrity, T. R. 1995. Dosimetric issues relating to particulate toxicity. *Inhal. Toxicol.* 7:615–632.
- Morgan, K. T., Patterson, D. L., and Gross, E. A. 1984. Frog palate mucociliary apparatus: Structure, function, and response to formaldehyde gas. *Fundam. Appl. Toxicol.* 4:58–68.
- Morgan, K. T., Patterson, D. L., and Gross, E. A. 1986. Responses of the nasal mucociliary apparatus to airborne irritants. In *Toxicology of the nasal passages*, ed. C. S. Barrow, pp. 123–133. Washington, DC: Hemisphere.
- Morgan, K. T., Kimbell, J. S., Monticello, T. M., Patra, A. L., and Fleishman, A. 1991. Studies of inspiratory airflow patterns in the nasal passages of the F-344 rat and rhesus monkey using nasal molds: Relevance to formaldehyde toxicity. *Toxicol. Appl. Pharmacol.* 110:223–240.
- Morrow, P. E. 1988. Possible mechanisms to explain dust overloading of the lungs. *Fundam. Appl. Toxicol.* 10:369–384.
- Morrow, P. E. 1992. Dust overloading of the lungs: Update and appraisal. *Toxicol. Appl. Pharmacol.* 113:1–12.
- Morrow, P. E. 1994. Mechanisms and significance of particle overload. In *Toxic and carcinogenic effects of solid particles in the respiratory tract* (ILSI Monograph), eds. U. Mohr, D. L. Dungworth, J. L. Mauderly, and G. Oberdörster, pp. 17–25. Washington, DC: ILSI Press.
- Muhle, H., Bellmann, B., Creutzenberg, O., Stöber, W., Kilpper, R., MacKenzie, J., Morrow, P., and Mermelstein, R. 1988. Pulmonary deposition, clearance and retention of test toner, TiO₂ and quartz during a long term inhalation study in rats. *Toxicologist* 8:69.
- Muhle, H., Bellmann, B., Creutzenberg, O., Heinrich, U., Ketkar, M., and Mermelstein, R. 1990a. Dust overloading of the lungs after exposure of rats to particles of low solubility: Comparative studies. *J. Aerosol. Sci.* 21:374–377.
- Muhle, H., Bellmann, B., Creutzenberg, O., Fuhst, R., Koch, W., Mohr, U., Takenaka, S., Morrow, P., Kilpper, R., MacKenzie, J., and Mermelstein, R. 1990b. Subchronic inhalation study of toner in rats. *Inhal. Toxicol.* 2:341–360.
- Muhle, H., Creutzenberg, O., Bellmann, B., Heinrich, U., and Mermelstein, R. 1990c. Dust overloading of lungs: Investigations of various materials, species differences, and irreversibility of effects. *J. Aerosol. Med.* 3(suppl. 1):111–128.
- Muhle, H., Bellmann, B., Creutzenberg, O., Dasenbrock, C., Ernst, H., Kilpper, R., MacKenzie, J. C., Morrow, P., Mohr, U., and Takenaka, S. 1991. Pulmonary response to toner upon chronic inhalation exposure in rats. *Fundam. Appl. Toxicol.* 17:280.
- Niinimaa, V., Cole, P., Mintz, S., and Shephard, R. J. 1981. Oronasal distribution of respiratory airflow. *Respir. Physiol.* 43:69–75.
- Oberdörster, G., Ferin, J., and Morrow, P. E. 1992. Volumetric loading of alveolar macrophages (AM): A possible basis for AM-mediated particle clearance. *Exp. Lung Res.* 18:87–104.

- Pattle, R. E. 1961. The retention of gases and particles in the human nose. In *Inhaled particles and vapours: Proceedings of an international symposium*, March–April 1960, Oxford, ed. C. N. Davis, pp. 302–311. New York: Pergamon Press.
- Phipps, R. J. 1981. The airway mucociliary system. In *Respiratory physiology III*, ed. J. G. Widdicombe, pp. 213–260. Baltimore, MD: University Park Press.
- Proctor, D. F., and Anderson, I., eds. 1982. *The nose, upper airway physiology and the atmospheric environment*. New York: Elsevier.
- Raabe, O. G. 1982. Deposition and clearance of inhaled aerosols. In *Mechanisms in respiratory toxicology*, ed. H. Witschi, pp. 27–76. Boca Raton, FL: CRC Press.
- Raabe, O. G., Al-Bayati, M. A., Teague, S. V., and Rasolt, A. 1988. Regional deposition of inhaled monodisperse, coarse, and fine aerosol particles in small laboratory animals. In *Inhaled particles VI: Proceedings of an international symposium and workshop on lung dosimetry*, September 1985, Cambridge, eds. J. Dodgson, R. I. McCallum, M. R. Bailey, and D. R. Fischer. *Ann. Occup. Hyg.* 32(suppl. 1):53–63.
- Rooney, S. A. 1992. Phospholipid composition, biosynthesis, and secretion. In *Comparative biology of the normal lung*, vol. 1, ed. R. A. Parent, pp. 511–544. Boca Raton, FL: CRC Press.
- Roy, M. 1989. Lung clearance modeling on the basis of physiological and biological parameters. *Health Phys.* 57(suppl. 1):255–262.
- Rudolph, G. 1975. Deposition von aerosolteilchen in der nase [Deposition of aerosol particles in the nose]. Diploma thesis, University Frankfurt/Main, Frankfurt, Federal Republic of Germany.
- Santa Cruz, R., Landa, J., Hirsch, J., and Sackner, M. A. 1974. Tracheal mucous velocity in normal man and patients with obstructive lung disease: Effects of terbutaline. *Am. Rev. Respir. Dis.* 109:458–463.
- Scheuch, G., and Stahlhofen, W. 1988. Particle deposition of inhaled aerosol boluses in the upper human airways. *J. Aerosol Med.* 1:29–36.
- Schlesinger, R. B. 1985. Comparative deposition of inhaled aerosols in experimental animals and humans: A review. *J. Toxicol. Environ. Health* 15:197–214.
- Schlesinger, R. B. 1988. Biological disposition of airborne particles: Basic principles and application to vehicular emissions. In *Air pollution, the automobile, and public health*, eds. A. Y. Watson, R. R. Bates, and D. Kennedy, pp. 239–298. Washington, DC: National Academy Press.
- Schlesinger, R. B. 1989. Deposition and clearance of inhaled particles. In *Concepts in inhalation toxicology*, eds. R. O. McClellan and R. F. Henderson, pp. 163–192. Washington, DC: Taylor & Francis.
- Schum, M., and Yeh, H. C. 1980. Theoretical evaluation of aerosol deposition in anatomical models of mammalian lung airways. *Bull. Math. Biol.* 42:1–15.
- Snipes, M. B. 1989. Long-term retention and clearance of particles inhaled by mammalian species. *Rev. Toxicol.* 20:175–211.
- Snipes, M. B. 1995. Pulmonary retention of particles and fibers: Biokinetics and effects of exposure concentration. In *Concepts in inhalation toxicology*, eds. R. O. McClellan and R. F. Henderson, pp. 225–255. Washington, DC: Taylor & Francis.
- Snipes, M. B., and Clem, M. F. 1981. Retention of microspheres in the rat lung after intratracheal instillation. *Environ. Res.* 24:33–41.
- Snipes, M. B., Boecker, B. B., and McClellan, R. O. 1983. Retention of monodisperse or polydisperse aluminosilicate particles inhaled by dogs, rats, and mice. *Toxicol. Appl. Pharmacol.* 69:345–362.
- Soong, T. T., Nicholaides, P., Yu, C. P., and Soong, S. C. 1979. A statistical description of the human tracheobronchial tree geometry. *Respir. Physiol.* 37:161–172.
- Stahlhofen, W., Gebhart, J., and Heyder, J. 1980. Experimental determination of the regional deposition of aerosol particles in the human respiratory tract. *Am. Ind. Hyg. Assoc. J.* 41:385–398a.
- Stahlhofen, W., Gebhart, J., and Heyder, J. 1981. Biological variability of regional deposition of aerosol particles in the human respiratory tract. *Am. Ind. Hyg. Assoc. J.* 42:348–352.
- Stahlhofen, W., Gebhart, J., Heyder, J., and Scheuch, G. 1983. New regional deposition data of the human respiratory tract. *J. Aerosol Sci.* 14:186–188.

- Stahlhofen, W., Gebhart, J., Rudolf, G., and Scheuch, G. 1986. Measurement of the lung clearance with pulses of radioactively-labelled aerosols. *Aerosol Sci.* 17:333–336.
- Stahlhofen, W., Rudolf, G., and James, A. C. 1989. Intercomparison of experimental regional aerosol deposition data. *J. Aerosol Med.* 2:285–308.
- Stephens, R. J., Sloan, M. F., Evans, M. J., and Freeman, J. 1974. Early response of lung to low levels of ozone. *Am. J. Pathol.* 74:31–58.
- Stöber, W. 1972. Dynamic shape factors of nonspherical aerosol particles. In *Assessment of airborne particles*, eds. T. T. Mercer, P. E. Morrow, and W. Stöber, pp. 249–289. Springfield, IL: C. C. Thomas.
- Stöber, W., and Mauderly, J. L. 1994. Model-inferred hypothesis of a critical dose for overload tumor induction by diesel soot and carbon black. *Inhal. Toxicol.* 6:427–457.
- Stöber, W., and McClellan, R. O. 1997. Pulmonary retention and clearance of inhaled biopersistent aerosol particles: Data-reducing interpolation models and models of physiologically based systems—A review of recent progress and remaining problems. *Crit. Rev. Toxicol.* 27:539–598.
- Stöber, W., Morrow, P. E., and Hoover, M. D. 1989. Compartmental modeling of insoluble particles deposited in the alveolar region of the lung. *Fundam. Appl. Toxicol.* 13:823–842.
- Stöber, W., Morrow, P. E., and Morawietz, G. 1990a. Alveolar retention and clearance of insoluble particles in rats simulated by a new physiologically-oriented compartmental kinetics model. *Fundam. Appl. Toxicol.* 15:329–349.
- Stöber, W., Morrow, P. E., Morawietz, G., Koch, W., and Hoover, M. D. 1990b. Development in modeling alveolar retention of insoluble particles in rats. *J. Aerosol Med.* 3(suppl. 1):S129–S154.
- Stöber, W., Morrow, P. E., Koch, W., and Morawietz, G. 1994. Alveolar clearance and retention of insoluble particles in rats simulated by a model inferring macrophage particle load distribution. *J. Aerosol Sci.* 25:975–1002.
- Stöber, W., Miller, F. J., and McClellan, R. O. 1998. Requirements for a credible extrapolation model derived from health effects in rats exposed to particulate air pollution: A way to minimize the risks of human risk assessment? *Appl. Occup. Environ. Hyg.* 13:421–431.
- Stone, K. C., Mercer, R. R., Gehr, P., Stockstill, B., and Crapo, J. D. 1992. Allometric relationships of cell numbers and size in the mammalian lung. *Am. J. Respir. Cell Mol. Biol.* 6:235–243.
- Subramaniam, R. P., Richardson, R. B., Morgan, K. T., Kimbell, J. S., and Guilmette, R. A. 1998. Computational fluid dynamics simulations of inspiratory airflow in the human nose and nasopharynx. *Inhal. Toxicol.* 10:91–120.
- Takahashi, S., Kubota, Y., and Hatsuno, H. 1992. Effect of size on the movement of latex particles in the respiratory tract following local administration. *Inhal. Toxicol.* 4:113–123.
- U.S. Environmental Protection Agency. 1996. Dosimetry of inhaled particles in the respiratory tract. In *Air quality criteria for particulate matter*, vol. II, pp. 10-1–10c-24. Research Triangle Park, NC: National Center for Environmental Assessment.
- van As, A., and Webster, I. 1972. The organization of ciliary activity and mucus transport in pulmonary airways. *S. Afr. Med. J.* 46:347–350.
- van As, A., and Webster, I. 1974. The morphology of mucus in mammalian pulmonary airways. *Environ. Res.* 7:1–12.
- van Ree, J. H. L., and van Dishoeck, H. A. E. 1962. Some investigations on nasal ciliary activity. *Pract. Otorhinolaryngol.* 24:383–390.
- Warheit, D. B., Overby, L. H., George, G., and Brody, A. R. 1988. Pulmonary macrophages are attracted to inhaled particles through complement activation. *Exp. Lung Res.* 14:51–66.
- Weibel, E. R. 1963. *Morphometry of the human lung*. New York: Academic Press.
- Wolff, R. K. 1992. Mucociliary function. In *Comparative biology of the normal lung*, vol. 1, ed. R. A. Parent, pp. 659–680. Boca Raton, FL: CRC Press.
- Wolff, R. K., and Muggenburg, B. A. 1979. Comparison of two methods of measuring tracheal mucous clearance in anesthetized beagle dogs. *Am. Rev. Respir. Dis.* 120:137–142.
- Wolff, R. K., Henderson, R. F., Snipes, M. B., Griffith, W. C., Mauderly, J. L., Cuddihy, R. H., and McClellan, R. O. 1987. Alterations in particle accumulation and clearance in lungs of rats chronically exposed to diesel exhaust. *Fundam. Appl. Toxicol.* 9:154–166.

- Xu, G. B., and Yu, C. P. 1987. Deposition of diesel exhaust particles in mammalian lungs: A comparison between particles in a human nasal cast. *Inhal. Toxicol.* 1:1-11.
- Yeates, D. B., Aspin, N., Levison, H., Jones, M. T., and Bryan, A. C. 1975. Mucociliary tracheal transport rates in man. *J. Appl. Physiol.* 39:487-495.
- Yeh, H.-C., and Harkema, J. R. 1993. Gross morphometry of airways. In *Toxicology of the lung*, 2d ed., D. L. Gardner, J. D. Crapo, and R. O. McClellan, eds., pp. 55-79. New York: Raven Press.
- Yeh, H. C., and Schum, G. M. 1980. Models of human lung airways and their application to inhaled particle deposition. *Bull. Math. Biol.* 42:461-480.
- Yeh, H. C., Schum, G. M., and Duggan, M. T. 1979. Anatomic models of the tracheobronchial and pulmonary regions of the rat. *Anat. Rec.* 195:483-492.
- Yoneda, K. 1976. Mucous blanket of rat bronchus. *Am. Rev. Respir. Dis.* 114:837-842.
- Yu, C. P., and Diu, C. K. 1983. Total and regional deposition of inhaled aerosols in humans. *J. Aerosol Sci.* 5:599-609.